

16

Soft Gamma Repeaters and Anomalous X-ray Pulsars: Magnetar Candidates

P.M. Woods

*Universities Space Research Association
National Space Science and Technology Center
Huntsville, AL, USA*

C. Thompson

*Canadian Institute for Theoretical Astrophysics
60 St. George Street
Toronto, ON, Canada*

16.1 Introduction

Baade & Zwicky (1934) were the first to envision the formation of neutron stars as the end product of a supernova explosion. Their forward thinking was not vindicated for another three decades, with the discovery of the first radio pulsars by Bell and Hewish (Hewish et al. 1968). What Baade and Zwicky could not have anticipated, however, was the menagerie of astrophysical objects that are now associated with neutron stars. Today, we observe them as magnetically braking pulsars, accreting pulsars in binary systems, isolated cooling blackbodies, sources of astrophysical jets, and emitters of high-luminosity bursts of X-rays. Here, we focus on two of the most extraordinary evolutionary paths of a neutron star, namely Soft Gamma Repeaters (SGRs) and Anomalous X-ray Pulsars (AXPs).

Soft Gamma Repeaters were discovered as high-energy transient burst sources; some were later found also to be persistent X-ray pulsars, with periods of several seconds, that are spinning down rapidly. Anomalous X-ray Pulsars are identified through their persistent pulsations and rapid spin-down; some have also been found to emit SGR-like bursts. In spite of the differing methods of discovery, this convergence in the observed properties of the SGRs and AXPs has made it clear that they are, fundamentally, the same type of object. What distinguishes them from other neutron stars is the likely source of energy for their radiative emissions, magnetism. The cumulative behavior of SGRs and AXPs is now best described by the magnetar model, in which the decay of an ultrastrong magnetic field ($B > 10^{15}$

G) powers the high-luminosity bursts and also a substantial fraction of the persistent X-ray emission.

For many years, the apparent absence of radio pulsars with magnetic fields much exceeding 10^{13} G, and the apparent lack of a good motivation for the existence of much stronger fields in neutron stars, inhibited serious consideration of their astrophysical consequences. It was noted early on that fields as strong as $10^{14} - 10^{15}$ G could be present in neutron stars as the result of flux conservation from the progenitor star (Woltjer 1964). Ultrastrong magnetic fields were introduced by hand in simulations of rotating supernova collapse, as a catalyst for energetic outflows (LeBlanc & Wilson 1970; Symbalisty 1984). A related possibility is that ordinary radio pulsars could contain intense toroidal magnetic fields as a residue of strong differential rotation in the nascent neutron star (e.g. Ardelyan et al. 1987). Later it was realized that appropriate conditions for true dynamo action could exist in proto-neutron stars (Thompson & Duncan 1993), leading to the formation of a class of ultramagnetic neutron stars with dissipative properties distinct from those of radio pulsars (Duncan & Thompson 1992). In recent years, pulsar searches have largely closed the observational gap between the dipole fields of radio pulsars and magnetar candidates (Manchester 2004).

We first review the history of this relatively new subfield of high energy astrophysics. Then we summarize in more detail the burst emission, the persistent X-ray emission of the SGRs and AXPs, their torque behavior, the counterparts observed in other wavebands, and their associations with supernova remnants. Finally, we discuss the magnetar model.

16.1.1 Soft Gamma Repeaters: A brief history

On 1979 January 7, a burst of soft gamma-rays lasting a quarter of a second was detected from SGR 1806–20 by instruments aboard the *Venera* spacecraft – the first observation of a Soft Gamma Repeater. This burst, along with a handful like it recorded over the next few years, were originally classified as a subtype of classical Gamma-Ray Burst (GRB), one with a short duration and a soft spectrum (Mazets & Golenetskii 1981). The locations of three repeaters were obtained from this early data set. It was not until after an intense reactivation of SGR 1806–20 in 1983, however, that the independent nature of these sources was fully appreciated (Hurley 1986; Laros et al. 1987). Their propensity to emit multiple bursts (no GRB has yet been shown to repeat); the deficit of high energy gamma-ray emission; and their similarity to each other merited designation as a new class of astrophysical transient.

The first detection of a SGR burst was soon followed, on 1979 March 5, by the most energetic SGR flare yet recorded (Mazets et al. 1979). This extraordinary event began with an extremely bright spike peaking at $\sim 10^{45}$ ergs s^{-1} (Golenetskii et al. 1984), followed by a 3 minute train of coherent 8 s pulsations whose flux decayed in a quasi-exponential manner (Feroci et al. 2001). The burst was well localized at the edge of the supernova remnant (SNR) N49 in the Large Magellanic Cloud, and its source is now identified as SGR 0526–66 (Cline et al. 1982). The high luminosity, strong pulsations, and apparent association with a SNR strongly suggested that the source was a young, magnetized neutron star with a spin period of 8 s.

Following the announcement of the SGRs, a variety of models were proposed. These included accretion onto magnetized neutron stars (e.g. Livio & Taam 1987; Katz, Toole & Unruh 1994), cometary accretion onto quark stars (Alcock, Farhi & Olinto 1986), as well as thermonuclear energy release on a magnetized neutron star (Woosley & Wallace 1982). Damping of the vibration of a neutron star had been suggested as a mechanism for the March 5 flare (Ramaty et al. 1980), but the coupling of the crust to the magnetosphere is much too weak to explain the observed luminosity if $B \sim 10^{12}$ G (Blaes et al. 1989). Indeed, the main shortcoming of all these models (e.g. Norris et al. 1991) was the lack of an adequate explanation for both the giant flare and the more common recurrent bursts, which last only ~ 0.1 s and have much lower peak luminosities ($< 10^{41}$ ergs s^{-1}).

Efforts to understand the nature of the SGRs were constrained by the lack of information about persistent counterparts. This changed with the discovery of persistent X-ray emission from all three known SGRs (Murakami et al. 1994; Rothschild, Kulkarni & Lingenfelter 1994; Vasisht et al. 1994). Around the same time, the magnetar model was put forth to explain the high-luminosity bursts of the SGRs (Duncan & Thompson 1992; Paczyński 1992; Thompson & Duncan 1995) and the persistent X-ray emission of both the SGRs and the AXPs (Thompson & Duncan 1996). Thompson & Duncan (1996) predicted slow pulsations and rapid spin down from the quiescent X-ray counterparts of the SGRs. A major breakthrough in determining the nature of SGRs was made shortly thereafter (Kouveliotou et al. 1998), with the discovery of 7.5 s pulsations and rapid spin down in the X-ray counterpart to SGR 1806–20. Kouveliotou et al. (1998) interpreted this measurement in terms of the magnetic braking of an isolated neutron star with a $\simeq 10^{15}$ G dipole magnetic field.

Our understanding of SGRs has continued to blossom in recent years in good part due to extensive monitoring campaigns and improved instrumentation. These observations have revealed correlated changes in SGR persis-

tent emission properties during periods of burst activity, dramatic variations in spindown torque, and a much larger collection of bursts of all types. For example, a near carbon-copy of the first giant flare was recorded on 1998 August 27 from SGR 1900+14 (Hurley et al. 1999a). In spite of detector advancements, there has been only one additional confirmed SGR discovered after the first three in 1979: SGR 1627–41 emitted more than 100 bursts in 1998 (Woods et al. 1999a). Two bursts were recorded in 1997 from a fifth candidate source, SGR 1801–23 (Cline et al. 2000). Another candidate, SGR 1808–20, was detected once and localized (Lamb et al. 2003a) to a position very near, but formally inconsistent with, the direction of SGR 1806–20. It should be cautioned that this burst was recorded during a burst active phase of SGR 1806–20. Note that we have not included in this tally sources first identified as AXPs, and later found to burst like SGRs.

16.1.2 Anomalous X-ray Pulsars: A brief history

The first detection of an Anomalous X-ray Pulsar was made by Fahlman & Gregory (1981), who discovered pulsations from the X-ray source 1E 2259+586 at the center of the SNR CTB 109. This object was first interpreted as a peculiar X-ray binary: its energy spectrum was much softer than is typical of accreting pulsars, and no optical counterpart was detected. Later the source was found to be spinning down in a secular manner (Koyama, Hoshi & Nagase 1987). Its X-ray luminosity was much too high to be powered by the loss of rotational energy from the putative neutron star.

Several other similar sources were discovered in the ensuing fifteen years. The objects 1E 2259+586, 1E 1048.1–5937, and 4U 0142+61 were grouped together by Hellier (1994) and Mereghetti & Stella (1995) as possible low-mass X-ray binaries, along with the known short-period binary 4U 1626–67. (The source RX J1838.4–0301 was also included initially, but was later shown not to be an X-ray pulsar.) The salient properties of this class were a narrow range of spin periods (5–9 s), fairly constant X-ray luminosities ($\sim 10^{35}$ – 10^{36} ergs s⁻¹), no evidence for orbital Doppler shifts and – with the exception of 4U 1626–67 – relatively soft X-ray spectra and steady spin down. However, 4U 1626–67 is also distinguished from the other sources by the detection of optical pulsations of the brightness expected from a compact, accreting binary. In light of these differences, its membership as an AXP has been revoked. Three new AXPs have been discovered since 1996 (1RXS J170849.0–400910, 1E 1841–045, and XTE J1810–197), along with two candidate sources (AX J1845–0258 and CXOU J0110043.1–721134).

The AXPs nonetheless appear to be too young to be low-mass binaries:

some are associated with SNR, and they have a small scale height above the Galactic plane (van Paradijs, Taam & van den Heuvel 1995). As noted by Thompson & Duncan (1993, 1996), their ‘anomalous’ property is the mechanism powering their X-ray emission. These authors identified 1E 2259+586, and later the AXP population as a whole, with isolated magnetars powered by the decay of a $\sim 10^{15}$ G magnetic field. The principal competing model postulated that the AXPs are neutron stars surrounded by fossil disks that were acquired during supernova collapse or during a common-envelope interaction (Corbet et al. 1995; van Paradijs et al. 1995; Chatterjee, Hernquist, & Narayan 2000; Chatterjee & Hernquist 2000). Finally, it was also noted that the loss of rotational energy from an isolated, magnetic, high-mass white dwarf is much larger than from a neutron star with the same spin parameters, and could supply the observed X-ray output (Paczynski 1990). However, the apparent youth of the object, and its residence in a SNR, remained puzzling in that interpretation.

The detection of optical and near infrared counterparts to the AXPs, beginning with 4U 0142+61 (Hulleman, van Kerkwijk & Kulkarni 2000), has provided a useful discriminant between the fossil disk and magnetar models. Dim counterparts have now been detected for four AXPs, with an optical/IR luminosity typically one thousandth of that emitted in 2–10 keV X-rays. This constrains any remnant accreting disk to be very compact (e.g. Perna, Hernquist & Narayan 2000). The optical emission of 4U 0142+61 has been found to pulse at the same period as in the X-ray band, with a pulsed fraction that is equal or higher (Kern & Martin 2002). The large pulsed fraction appears problematic in any accretion model, where the optical emission arises from reprocessing of the X-rays by a disk. There are no reliable *a priori* predictions of optical/infrared emission from magnetars.

The detection of X-ray bursts similar to SGR bursts from at least one, and possibly two, AXPs has confirmed a key prediction of the magnetar model. Two weak bursts were observed from the direction of 1E 1048.1–5937 (Gavriil, Kaspi & Woods 2002); and more than 80 SGR-like bursts were detected from 1E 2259+586 during a single, brief (~ 11 ks) observation of the source (Kaspi et al. 2003). Overall, at least 10 percent of the X-ray output of 1E 2259+586 appears to be powered by transient releases of energy, and a much larger fraction in some other AXPs. Although these observations have not yet provided unambiguous proof that the AXPs have ultrastrong magnetic fields, they have confirmed the conjecture that the AXPs and SGRs belong to the same class of neutron stars. In this review, we refer to these sources collectively as magnetar candidates.

16.2 Burst Observations

The defining behavior of SGRs is their repetitive emission of bright bursts of low-energy (soft) gamma-rays. The most common SGR bursts have short durations (~ 0.1 s), thermal spectra, and peak luminosities reaching up to 10^{41} ergs s^{-1} — well above the standard Eddington limit of $\sim 2 \times 10^{38}$ ergs s^{-1} for a $1.4 M_{\odot}$ neutron star. In this section, we describe these short bursts and the similar bursts detected from two AXPs. We then review the more extraordinary bursts emitted by the SGRs, including the two giant flares and the intermediate bursts. Unless otherwise stated, the quoted burst luminosities and energies cover photon energies above 20 keV and assume isotropic emission.

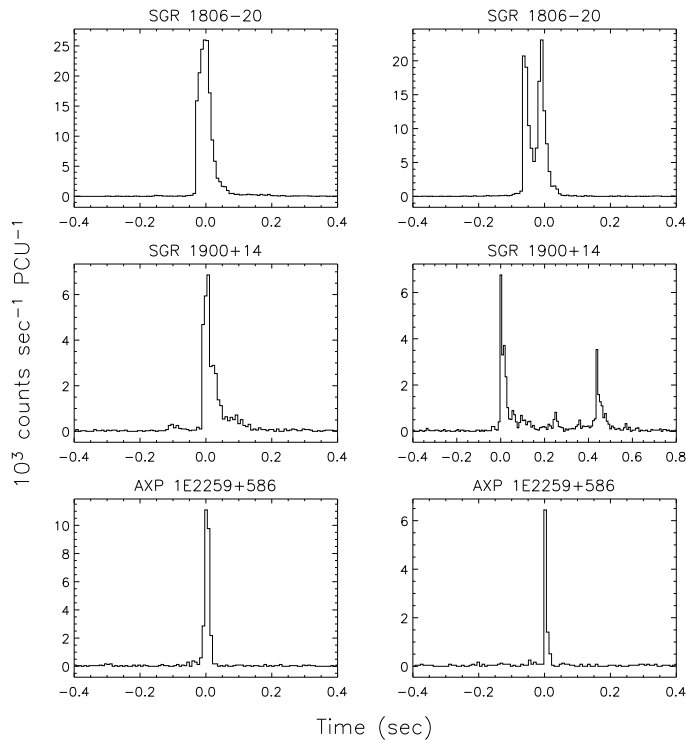


Fig. 16.1. A selection of common burst morphologies recorded from SGR 1806–20, SGR 1900+14 and 1E 2259+586, as observed with the *RXTE* PCA. All light curves display counts in the energy range 2–20 keV, with a time resolution of 7.8 ms. See text for further details.

16.2.1 Short Duration SGR Bursts: Temporal Properties

The properties of the most common SGR bursts do not appear to vary greatly between different periods of activity, or indeed between different sources (e.g. Aptekar et al. 2001; Göğüş et al. 2001). A burst typically has a faster rise than decay, and lasts ~ 100 ms. Four examples from SGR 1806–20, SGR 1900+14, and 1E 2259+586 are shown in Figure 16.1. A number of bursts are multi-peaked, like the two shown from SGR 1806–20 and SGR 1900+14. The intervals between sub-peaks have a broad distribution, suggesting that these multi-peaked bursts are a superposition of two (or more) single-peaked bursts close in time (Göğüş et al. 2001).

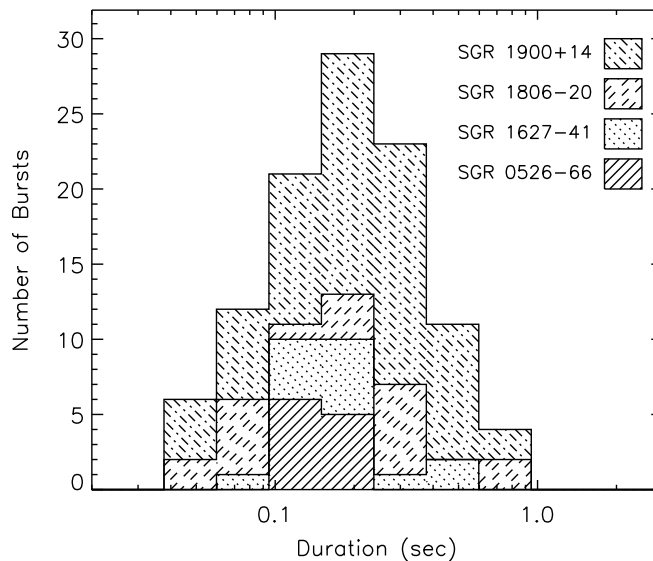


Fig. 16.2. Duration distribution for 106 bursts from the four known SGRs as observed by the Konus detectors (15–100 keV) between 1978 and 2000 (Aptekar et al. 2001).

The morphological uniformity of (the majority of) SGR bursts was noted early on (e.g. Atteia et al. 1987; Kouveliotou et al. 1987). The burst durations have a narrow distribution: they show a mild positive correlation with burst fluence (e.g. Göğüş et al. 2001), but do not vary significantly with photon energy. A sample of 164 bursts recorded from the four known SGRs by the Konus series of gamma-ray detectors is tabulated by Aptekar et al. (2001). Durations could be measured for 106 ordinary bursts (Figure 16.2), with a mean of 224 ms. More recently, the higher flux sensitivity of the *Rossi X-ray Timing Explorer* PCA has provided larger burst samples for

individual sources, at lower photon energies (2–20 keV vs. > 25 keV). In particular, T_{90} burst durations[†] were measured for 190, 455, and 80 bursts from the magnetar candidates SGR 1806–20, SGR 1900+14 (Göğüş et al. 2001), and 1E 2259+586 (Gavriil, Kaspi & Woods 2004), respectively. The mean durations of these samples were 162, 94, and 99 ms. That these values are somewhat lower than in the Konus sample may be due, in part, to the higher mean fluence of the Konus bursts.

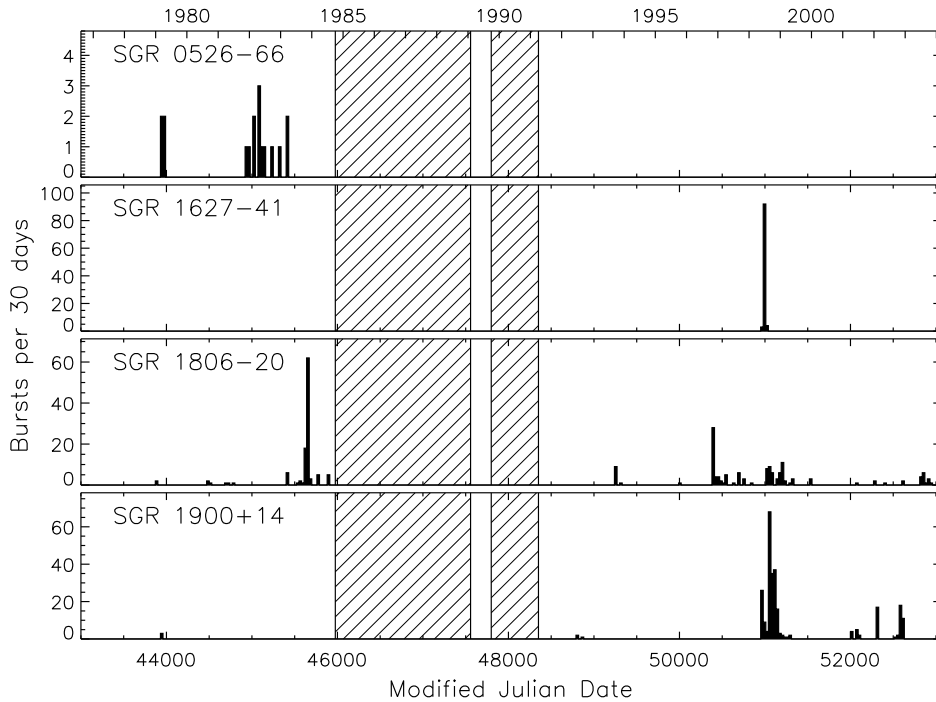


Fig. 16.3. Burst activity history of the four confirmed SGRs. The bursts identified here were detected with a suite of large field-of-view detectors having different sensitivities. The shaded regions indicate epochs where there were no active detectors sensitive to SGR bursts. IPN data courtesy of Kevin Hurley.

The burst activity in SGRs tends to be concentrated in time. These episodes of enhanced burst activity are referred to as outbursts. They occur at irregular intervals with variable duration and intensity (Figure 16.3). The recurrence patterns of individual bursts are just as irregular as those of the outbursts themselves, and differ dramatically from what is observed in X-ray bursts (of either Type I or II) in accreting neutron stars. There is no correlation between the energy of a given burst and the time to the

[†] The time to accumulate 90 percent of the burst fluence; see Koshut et al. (1996).

next burst in either the SGRs (Laros et al. 1987; Göğüş et al. 1999), or in 1E 2259+586 (Gavriil et al. 2004). (Such a correlation is present in the Type II bursts of the Rapid Burster; Chapter 8.)

The distribution of waiting times between bursts depends on the sensitivity of the detector and the strength of the outburst. The waiting times spanned some 7 orders of magnitude during the 1983 activation of SGR 1806–20 (Laros et al. 1987); and the distribution of waiting times was later found to follow a log-normal function with a mean of $\sim 10^4$ s (Hurley et al. 1994). The waiting times between bursts from SGR 1900+14, 1E 2259+586, and a more recent outburst of SGR 1806–20 are all distributed in a similar way, although given the lower flux threshold the mean waiting time is only $\sim 10^2$ s in these three samples.

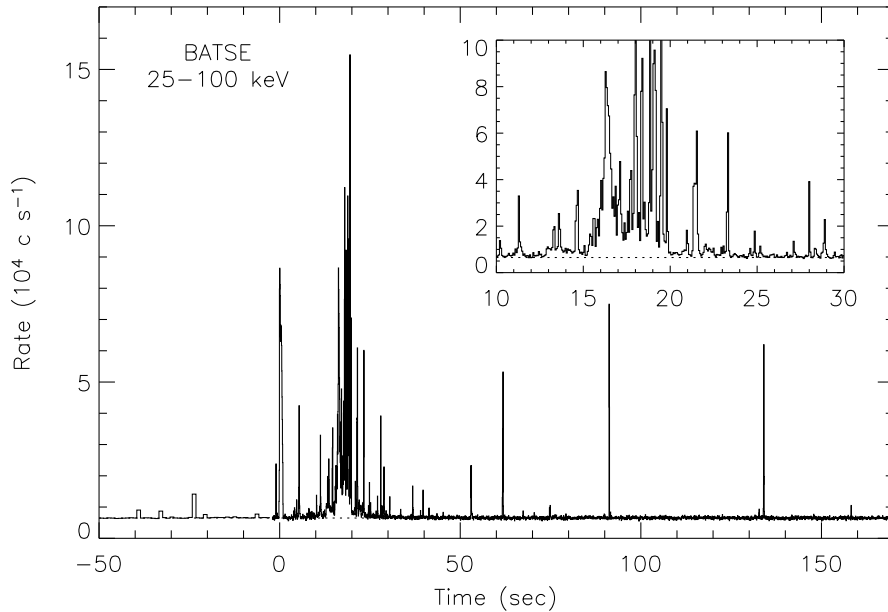


Fig. 16.4. The time history of the multi-episodic burst from SGR 1900+14 recorded on 1998 September 1 with BATSE (25–100 keV). The inset shows a close-up of the most intense part of the light curve. The background level is indicated by the dotted line. Note the envelope of emission lasting ~ 5 – 7 s during the most intense phase.

Series of many short bursts, with extremely small waiting times (multi-episodic bursts) have been observed on rare occasions (Hurley et al. 1999b). They involve several tens of bright SGR bursts which are packed into an interval of a few minutes. Intense burst episodes like these are more commonly

seen at lower peak flux; but three instances involving high luminosity SGR bursts have been recorded from SGR 1900+14. The BATSE light curve of the 1 September 1998 multi-episodic burst is shown in Figure 16.4. Note the continuous envelope of emission underlying the most intense portion of the burst episode.

16.2.2 Spectral Properties and Energy Distribution

Bursts from SGRs were discovered using all-sky detectors with little sensitivity below ~ 30 keV. Above this photon energy, SGR burst spectra are well modeled by optically thin thermal bremsstrahlung (OTTB). The temperatures so obtained fall within the narrow range $kT = 20 - 40$ keV, indicative of the spectral uniformity of SGR bursts. The spectra of SGR bursts vary weakly with intensity – not only from burst to burst within a given source, but also between sources. This effect was first demonstrated by Fenimore, Laros, & Ulmer (1994) for SGR 1806–20, and later by Aptekar et al. (2001) in the Konus sample of bursts from four SGR sources.

A typical SGR burst spectrum is compared (the solid line in Figure 16.5) with sample spectra from other extra-Solar high-energy burst phenomena. Although the soft end of the spectral distribution of GRBs and X-ray Flashes (XRFs) overlaps the SGRs, the durations of the SGR bursts are usually shorter by two orders of magnitude (see §16.2.1) and otherwise show strong morphological differences with GRBs. Distinguishing the two types of bursts is therefore straightforward in practice. One caveat here is that the initial ~ 0.3 -s spikes of the giant flares show greater spectral similarities with GRBs, and so a handful of extragalactic SGR flares may be hidden in the BATSE catalog of short-duration GRBs (Duncan 2001).

A shortcoming of the OTTB model is that it overpredicts the flux of photons with energies below ~ 15 keV (Fenimore et al. 1994). It is doubtful that this spectral rollover is due to a thick column of absorbing material, since the requisite N_{H} is an order of magnitude greater than what is deduced from the persistent X-ray emission. Recently, a 7 – 150 keV *HETE-2* spectrum of a high-fluence burst from SGR 1900+14 was successfully fit by the sum of 4.1 keV and 10.4 keV blackbodies (Olive et al. 2003). A similar result was obtained with 1.5 – 100 keV BeppoSAX spectra of 10 bursts also from SGR 1900+14 (Feroce et al. 2004). The temperatures of these lower peak flux bursts are consistent with the *HETE-2* burst spectrum – so that the flux ratio of the two blackbody components is approximately constant. Furthermore, the absorbing column measured during the bursts is consistent the value obtained in quiescence.

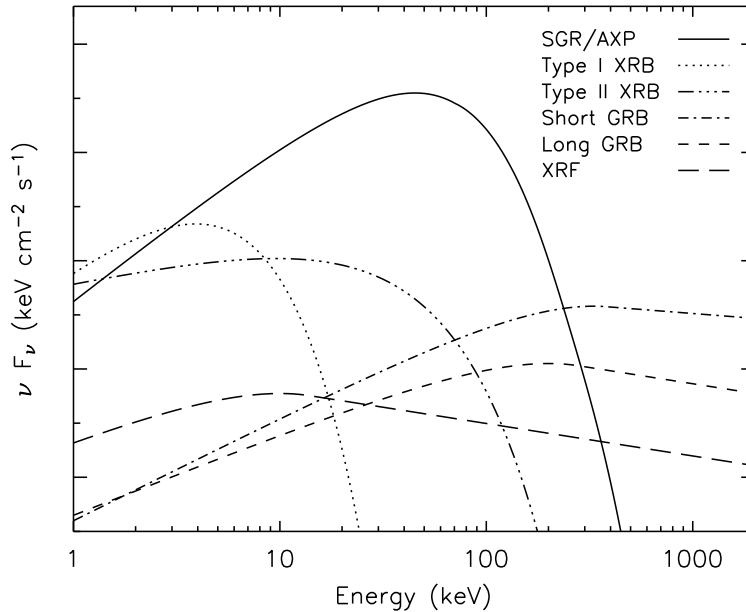


Fig. 16.5. Characteristic energy spectra of high-energy burst phenomena. The SGR/AXP (magnetar candidate) burst spectrum shown is a composite of the two blackbody model that fits burst spectra well below ~ 50 keV convolved with the OTTB model that better represents the burst spectrum at higher energies. Note that there exists a continuum of E_{peak} values between the softer XRFs and the harder/brighter long GRBs.

The improved sensitivity of *RXTE* allowed Göğüş et al. (2001) to show that the less energetic bursts from SGR 1806–20 and SGR 1900+14 are also slightly harder spectrally. The bursts detected from the AXP 1E 2259+586 have similar spectra to those of the SGRs, although in the AXP it is the brighter bursts which tend to be harder (Gavriil et al. 2004).

The energies radiated during the common (~ 0.1 -s) SGR bursts follow a power-law distribution, $dN/dE \propto E^{-5/3}$. Cheng et al. (1996) first uncovered this distribution in SGR 1806–20, and pointed out the similarity with the Gutenberg-Richter law for earthquakes. Similar distributions are measured in a variety of other physical systems, including Solar flares and avalanches. Subsequently, it has been shown that the other three SGRs and the AXP 1E 2259+586 all possess very similar burst energy distributions. The power-law index is about $-5/3$ in SGR 1900+14, SGR 1627–41, and 1E 2259+586, but is not well constrained in SGR 0526–66. A possible break from a $-5/3$ index to a somewhat flatter value (-1.4) at low burst energies was measured in a larger sample of bursts from SGR 1806–20 (Göğüş et al. 1999).

16.2.3 Giant Flares

Giant flares are the most extreme examples of SGR bursts. Their output of high energy photons is exceeded only by blazars and cosmological gamma-ray bursts, and their luminosity peaks above a million times the Eddington luminosity of a neutron star. The flares begin with a ~ 1 second spike of spectrally hard emission which decays rapidly into a softer, pulsating tail that persists for hundreds of seconds. These coherent pulsations are at the spin period of the underlying neutron star. The giant flares are rare: only two have been detected from the four known SGRs over 20 years of observation, so the corresponding rate is approximately once per 50–100 yrs (per source).

The first giant flare was recorded on 1979 March 5 from SGR 0526–66 (Mazets et al. 1979) and, indeed, was only the second SGR burst observed. The source is well localized in the LMC (§16.6), and so the isotropic energy of the flare was 5×10^{44} ergs – some thousand times larger than a typical thermonuclear flash. The initial peak of this flare lasted ~ 0.2 s and had significant structure on time scales shorter than ~ 2 ms. It was spectrally harder ($kT \sim 250 - 500$ keV) than the common SGR bursts, and reached a peak luminosity of 4×10^{44} ergs s^{-1} (Mazets et al. 1979; Fenimore et al. 1981). Thereafter, the flux decayed in a quasi-exponential manner over the next ~ 2 -3 minutes. A reanalysis of the *ISEE-3* data using a model of a magnetically confined, cooling fireball (see §16.7.2), shows that the data are also consistent with a well-defined termination of the X-ray flux at ~ 160 s (Feroci et al. 2001). The pulsations during this phase of the burst have a period of 8.00 ± 0.05 s (Terrell et al. 1980). The pulse profile shows two clear peaks per cycle and a change in morphology during the first few cycles. The spectrum of the decaying tail had an OTTB temperature of $\sim 30 - 38$ keV, consistent with the spectra of the recurrent burst emissions from this SGR.

The second giant flare was not recorded until almost 20 years later, on 1998 August 27 from SGR 1900+14 (Hurley et al. 1999a; Feroci et al. 1999; Mazets et al. 1999a; Feroci et al. 2001). This event (Figure 16.6) was, in many respects, a carbon copy of the March 5 flare. It began with a bright spike lasting ~ 0.35 s, and the X-ray spectrum contained a very hard power-law component $dN/dE \propto E^{-1.5}$ in the initial stages. Only a lower bound of 3×10^{44} ergs s^{-1} was obtained for its peak luminosity, because the flare saturated every detector that observed it. In fact, it was the brightest extra-Solar gamma-ray transient yet recorded. The X-ray flux incident on the night side of the Earth was high enough to force the ionosphere to its day-time level (Inan et al. 1999).

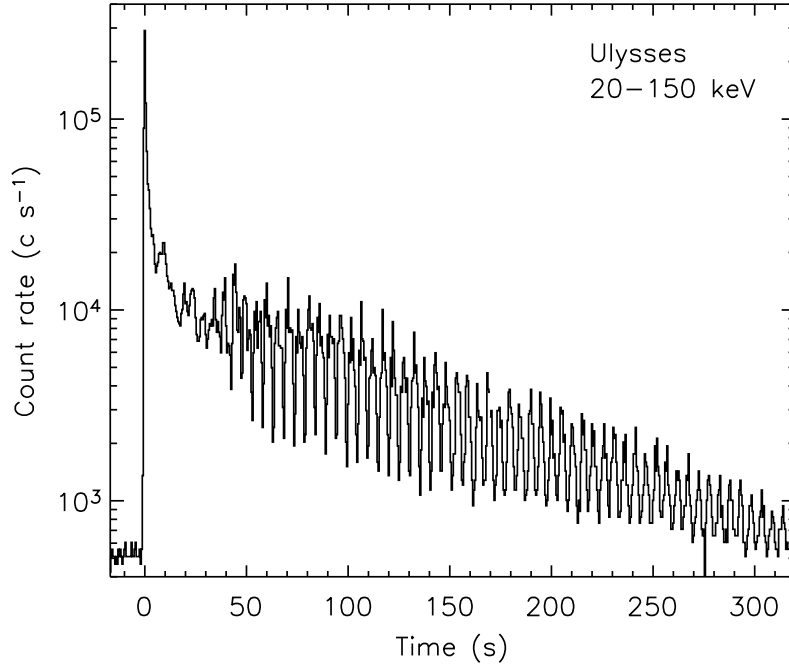


Fig. 16.6. The giant flare from SGR 1900+14 as observed with the gamma-ray detector aboard Ulysses (20–150 keV). Note the strong 5.16 s pulsations clearly visible during the decay. Data courtesy of Kevin Hurley.

In contrast with the previous flare, the decline in the flux from the August 27 flare was followed to a well-defined termination some 400 s after the initial spike (Feroci et al. 2001). The spectrum after the first 50 s equilibrated to a (OTTB) temperature of ~ 30 keV, even while the luminosity continued to decrease by more than an order of magnitude. During this same phase, the light curve maintained large-amplitude pulsations with a 5.16 s period, precisely equal to the periodicity that had been previously detected in the persistent X-ray emission of SGR 1900+14 (Hurley et al. 1999c). The pulse maintained a complex four-peaked pattern that gradually simplified into a smooth single pulse during the final stages of the flare (Mazets et al. 1999a).

16.2.4 Intermediate Bursts

Intermediate bursts are intermediate in duration, peak luminosity and energy between the common recurrent SGR bursts and the giant flares. SGR bursts which last longer than a second (but less than the rotation period of several seconds) tend to have abrupt onsets and end points, while their

flux varies modestly in between. By contrast, the light curves of the short, recurrent bursts (e.g. Göğüş et al. 2001) are usually more irregular, which suggests that the emitting particles cool more rapidly.

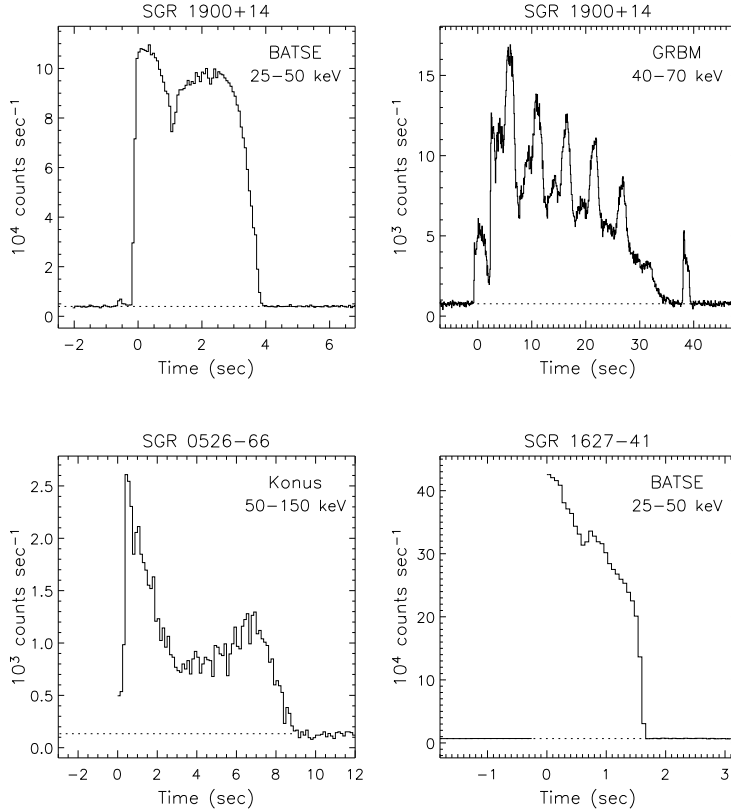


Fig. 16.7. Time histories of four intermediate bursts recorded from three of the four SGRs. Clockwise from upper left: SGR 1900+14 burst recorded with BATSE on 1998 October 28, SGR 1900+14 burst recorded with GRBM on 2001 April 18, SGR 1627-41 burst recorded with BATSE on 1998 June 18, and SGR 0526-66 burst recorded with Konus on 1982 February 27. Energy ranges are shown in each figure panel. The rise of the SGR 1627-41 burst is unresolved due to a gap in the BATSE data. GRBM data courtesy of M. Feroci and F. Frontera. Konus data courtesy of S. Golenetskii.

Time histories of four examples of intermediate bursts are shown in Figure 16.7. Their durations range from ~ 1 to 40 s and their isotropic energies from 10^{41} – 10^{43} ergs. Up until 1998, there were few intermediate bursts recorded from SGRs, most from SGR 0526-66 (Golenetskii et al. 1984). Since 1998, several more bursts have been detected from other SGRs which begin to fill in the apparent gap in energy and duration. (The largest was an

event recorded on 2001 April 18 from SGR 1900+14; Guidorzi et al. 2004.) This suggests that there may be a continuum of burst sizes covering the smallest recurrent bursts all the way up to the giant flares.

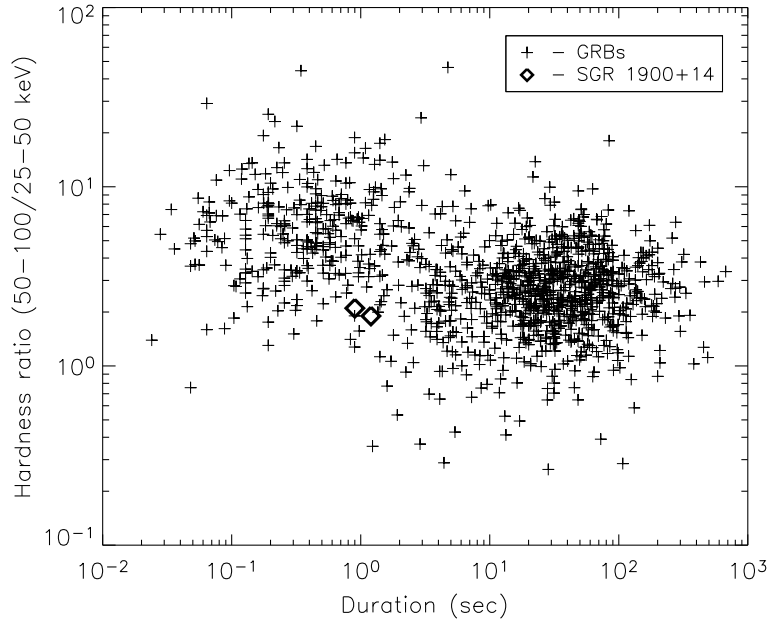


Fig. 16.8. Hardness ratio versus T_{90} duration for all GRBs (plus signs) in the BATSE 4B catalog (Paciesas et al. 2000) and the two spectrally hard SGR 1900+14 bursts (diamonds) detected with BATSE (Woods et al. 1999b).

The spectra of most intermediate bursts are consistent with the spectra of the short, recurrent bursts and the pulsating tails of the giant flares. The spectrum does not vary much, either from burst to burst or within individual bursts. A striking exception to this rule was a very intense ($L_{\text{peak}} \sim 10^{43}$ ergs s^{-1}) and spectrally hard ($kT_{\text{peak}} \sim 120$ keV) burst detected from SGR 1627–41 (Mazets et al. 1999b; Woods et al. 1999a). This burst lasted ~ 0.5 s and was similar both spectrally and temporally to the initial peaks of the giant flares – but without the extended softer pulsations. Two bursts recorded from SGR 1900+14 during the 1998–1999 activation were also spectrally much harder than all other burst emission from this SGR (Woods et al. 1999b) with the exception of the initial spike of the August 27 flare. These bursts are, in fact, spectrally and temporally indistinguishable from classical GRBs (Figure 16.8). They were not exceptionally

bright and had durations lasting ~ 1 s with a fast rise and exponential decay. Their spectra were consistent with a power law (photon index ~ -2) whose hardness was anti-correlated with X-ray flux.

16.2.5 Possible Spectral Features

Discrete features in burst spectra from magnetar candidates have been reported from SGR 0526–66, SGR 1900+14, SGR 1806–20, and 1E 1048.1–5937. It should be emphasized that, as was the case previously with classical gamma-ray bursts, the same spectral feature has not yet been detected in the same burst by independent instruments.

In SGR 0526–66, Mazets et al. (1979) reported evidence for a broad peak in the energy spectrum at ~ 430 keV during the main peak of the giant flare of March 5. Using *RXTE* PCA data, Strohmayer & Ibrahim (2000) discovered a significant emission feature at ~ 6.7 keV during a pre-cursor to the intermediate burst of 1998 August 29 from SGR 1900+14. An additional feature consistent with twice this energy is seen, but its significance is marginal. Ibrahim, Swank & Parke (2003) presented the analysis of 56 spectra accumulated with the *RXTE* PCA taken from selected SGR 1806–20 bursts intervals. Of the 56 spectra, a handful showed a statistically significant ($> 3\sigma$) absorption feature near 5 keV and much less significant features at integer multiples of this energy. These authors have argued that these lines represent proton cyclotron absorption features in a strong magnetic field. In addition, two bursts were recorded with the PCA from the direction of 1E 1048.1–5937 within two weeks of each other late in 2001 (Gavriil et al. 2002). In the first of these bursts, a strong emission feature was seen at ~ 7 keV with less significant features at energies consistent with the first three harmonics.

16.3 Persistent X-ray Emission

Historically, one of the defining properties of AXPs was the relative steadiness of their X-ray emission, over a fairly narrow range $10^{35} - 10^{36}$ ergs s^{-1} . Over the last several years, however, it has become clear that at least half and possibly most magnetar candidates are variable X-ray sources. Some of the observed variability is clearly driven by burst activity (see §16.5), but at least a few sources have shown large changes in luminosity ($\sim 10-100$) with little or no detected burst activity. For example, XTE J1810–197 was discovered in 2003 at a luminosity of $\sim 2 \times 10^{36}$ ergs s^{-1} (Ibrahim et al. 2004), but archival observations from the 1990’s found the source in a “low

state” with a luminosity two orders of magnitude smaller (Gotthelf et al. 2004). One of the AXP candidates, AX J1845–0258, was discovered at a luminosity $\sim 10^{35}$ ergs s^{-1} in a 1993 *ASCA* observation (Torii et al. 1998; Gotthelf & Vasisht 1998), yet follow-up observations 3 and 6 years later found the flux 20 times dimmer (Vasisht et al. 2000). No SGR-like bursts have ever been seen from either of these sources.

One of the best studied AXPs, 1E 1048.1–5937, has also shown signs of flux variability (e.g. Oosterbroek et al. 1998). Weekly monitoring with *RXTE* has revealed two pulsed flux flares lasting several months (Gavriil & Kaspi 2004). Unlike the burst induced variability, the rises of these flares were resolved lasting a few weeks. Interestingly, two small bursts were detected near the peak of the first flare (Gavriil et al. 2002), but none were seen at any point during the much brighter and longer-lived second flare. Imaging X-ray observations have shown similar variability in the phase-averaged luminosity, albeit with much sparser sampling (Mereghetti et al. 2004). As with XTE J1810–197 and AX J1845–0258, the “baseline” luminosity of 1E 1048.1–5937 is low ($\sim 6 \times 10^{33}$ ergs s^{-1}) relative to the average luminosity of the AXP class.

The realization that SGRs and AXPs can enter low states with luminosities of order $10^{33} - 10^{34}$ ergs s^{-1} for extended periods of time has important implications on the total number density of magnetar candidates in our Galaxy (§16.8). Their duty cycle as bright X-ray sources is presently unknown, especially as a function of the age. There is still much to be learned about the similarities and differences between magnetar candidates in their dim states, and other low-luminosity X-ray sources such as Isolated Neutron Stars, Compact Central Objects and high-field radio pulsars. It is possible that some of these other sources occasionally become X-ray bright like the AXPs (§16.6.3).

16.3.1 X-ray Spectra

The X-ray spectra of SGRs and AXPs (0.5–10 keV) are usually well fit by a two-component model, a blackbody plus a power law, modified by interstellar absorption (Table 16.1). The soft blackbody component is not required in a few sources, but these tend to be dim and/or heavily absorbed (e.g. SGR 1627–41). During quiescence (i.e., outside of bursting activity), the blackbody temperature does not vary greatly between different members of the class (Marsden & White 2001) or with time for individual sources (e.g. Oosterbroek et al. 1998). On the other hand, the non-thermal component

does show significant variations between different sources (Marsden & White 2001) and with time in a few cases (e.g. Woods et al. 2004).

Table 16.1. *X-ray spectral properties of the SGRs and AXPs.*

Source ^a	N _H 10 ²² (cm ⁻²)	Blackbody Temperature (keV)	Photon Index	Unabsorbed ^b Flux 10 ⁻¹¹ (ergs cm ⁻² s ⁻¹)	Luminosity ^c 10 ³⁵ (ergs s ⁻¹)
SGR 0526–66	0.55	0.53	3.1	0.087	2.6
SGR 1627–41	9.0	–	2.9	0.027–0.67	0.04–1.0
SGR 1806–20	6.3	–	2.0	1.2–2.0	3.2–5.4
SGR 1900+14	2.6	0.43	1.0–2.5	0.75–1.3	2.0–3.5
CXOU 010043.1–721134	0.14	0.41	–	0.010	0.39
4U 0142+61	0.91	0.46	3.4	8.3	0.72
1E 1048.1–5937	1.0	0.63	2.9	0.41–2.3	0.053–0.25
1RXS J170849–400910	1.4	0.44	2.4	6.4	1.9
XTE J1810–197 ^d	1.1	0.67	3.7	0.01–2.2	0.01–2.6
1E 1841–045	2.5	0.44	2.0	1.9	1.1
AX J1845–0258	9	–	4.6	0.04–1.0	0.05–1.2
1E 2259+586	1.1	0.41	3.6–4.2	1.6–5.5	0.17–0.59

a – Spectral values given for quiescent state only (i.e. periods with no *detected* burst activity)

b – All fluxes and luminosities integrated over 2.0–10.0 keV

c – Assumed distances given in Table 16.4

d – Spectral parameters given were obtained during “high” state of source following its discovery in 2003

REFERENCES – (SGR 0526) Kulkarni et al. 2003; (SGR 1627) Kouveliotou et al. 2003; (SGR 1806) Mereghetti et al. 2000; (SGR 1900) Woods et al. 2001; (CXO 0100) Lamb et al. 2002; (4U 0142) Patel et al. 2003; (1E 1048) Mereghetti et al. 2004; (RXS 1708) Rea et al. 2003; (XTE 1810) Gotthelf et al. 2004; (1E 1841) Morii et al. 2003; (AX 1844) Gotthelf & Vasisht 1998, Torii et al. 1998, Vasisht et al. 2000; (1E 2259) Woods et al. 2004

The first systematic study of the X-ray spectra of SGRs and AXPs was performed by Marsden & White (2001), who found that the spectral hardness of the persistent X-ray counterparts of these sources formed a continuum and was positively correlated with the spin-down rate of the pulsar (Figure 16.9). The varying hardness of the X-ray spectrum with spin-down rate was linked to the non-thermal component of the spectrum.

Very little is known about the X-ray spectra of magnetar candidates above ~10 keV due to the limitations of past and current instrumentation. The

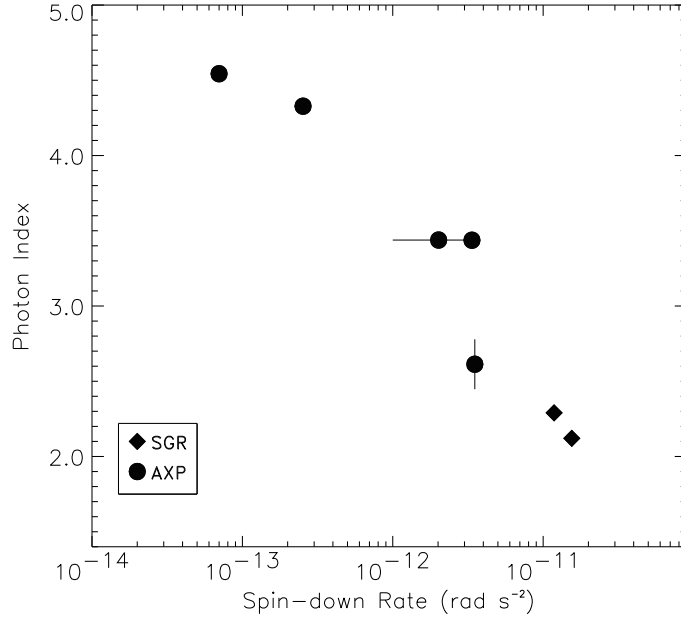


Fig. 16.9. The variation of the single power law photon index versus spin-down rate $|\dot{\Omega}|$ for each SGR and AXP. The results for objects with more than one observation have been averaged. The photon index decreases (spectral hardness increases) with increasing spin-down rate. Figure from Marsden & White (2001).

persistent emission of only one magnetar candidate, 1E 1841–045, has been securely detected above ~ 15 keV using *Integral* (Molkov et al. 2004) and *RXTE* HEXTE (Kuiper, Hermsen & Mendez 2004). At high energies, the spectrum follows a power law with a photon index -1.0 up to at least 100 keV. Knowledge of the photon distribution with energy above 15 keV is crucial to determining the underlying emission mechanism (see §16.7.4). More sensitive, imaging hard X-ray detector facilities such as *Integral* and *Swift* should lead to more detections at high energies.

There are no definite detections of spectral features in the *persistent* X-ray emission of magnetar candidates. Grating spectra from *Chandra* and *XMM-Newton* have yielded strong upper limits (< 30 eV) on narrow line features for 4U 0142+61 (Juett et al. 2002) and 1E 2259+586 (Woods et al. 2004) in the energy range 0.5–5 keV. The only reported detection of a spectral feature comes from a *BeppoSAX* spectrum of 1RXS J170849.0–400910 where Rea et al. (2003) find a $\sim 4\sigma$ excess (i.e. emission line) at ~ 8 keV. The absence of spectral features at X-ray energies where proton-cyclotron resonances would

occur in magnetar-strength fields places strong constraints on models of the transmission of heat through the surface, and of surface heating.

16.3.2 Pulse Profiles and Pulsed Fractions

The X-ray pulse profiles of magnetar candidates range from simple half-sinusoids to more complex profiles showing (typically) two maxima per cycle (Figure 16.10). The observed pulse morphologies of the AXPs are consistent with either one or two hotspots on the surface of a neutron star (Özel 2002), but the spectrally harder SGRs sometimes have more complicated pulse profiles. In contrast with most accreting X-ray pulsars, the pulse profile of a SGR or AXP often has a weak dependence on photon energy.

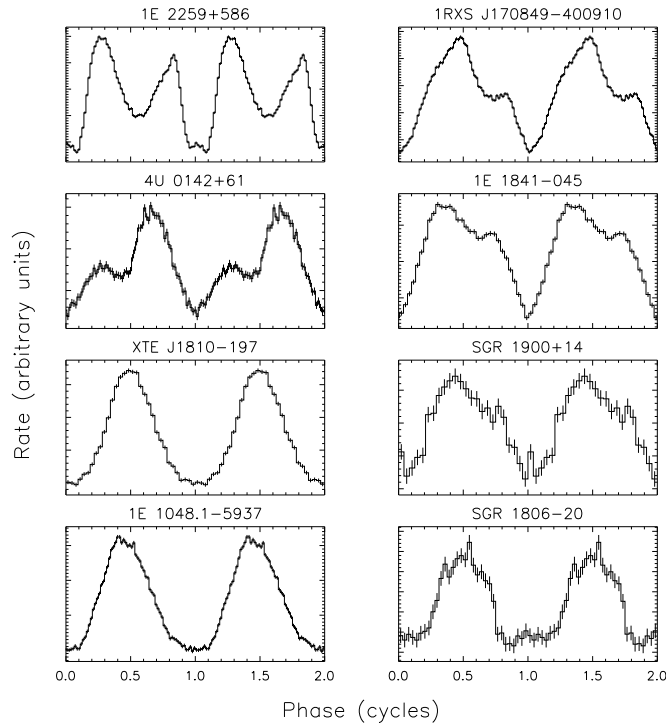


Fig. 16.10. The folded pulse profiles of eight different magnetar candidates. The sources are ranked according to inferred dipole magnetic field strength. Magnetic field increases from top to bottom and left to right. All profiles are of X-rays between 2 and 10 keV as observed with the *RXTE* PCA. Note that the folded profile of SGR 1900+14 is from after the August 27 flare. AXP pulse profiles courtesy of V.M. Kaspi and F.P. Gavriil.

The pulse profiles shown in Figure 16.10 are ranked in order of increasing

spin-down rate (from top to bottom and left to right). No strong trend is apparent; but note that the pulse profile of SGR 1900+14 was much more complex before the August 27 flare. The evolution of the pulse morphology in SGR 1900+14 and other magnetar candidates is discussed in §16.5.3.

The root-mean-square (rms) X-ray pulsed fractions of magnetar candidates range from 4 to 60% (Table 16.2). Note that in the literature, both peak-to-peak and rms are reported, and the rms values are always less than the peak-to-peak values for any given AXP/SGR pulse profile. Similar to the pulse shape, the pulsed fractions of the AXPs show little or no change with photon energy (0.5–10 keV). Since the relative contribution of the blackbody spectral component to the total photon flux changes from 0% to as much as $\sim 70\%$ over this bandpass, Özel, Psaltis & Kaspi (2001) argued that the two spectral components of the AXPs must be highly correlated or caused by the same physical process.

16.4 Timing Behavior

The spin periods of the SGRs and AXPs are clustered between 5 and 12 seconds, a very narrow range compared with radio pulsars and accreting X-ray pulsars. These sources are all spinning down rapidly and persistently, with fairly short characteristic ages $P/\dot{P} \sim 10^3 - 10^5$ yrs. The magnitude of the spindown torque is consistent with magnetic dipole braking of an isolated neutron star with a dipole field of $\sim 10^{14} - 10^{15}$ G (Figure 16.11). Although most of the characteristic ages are less than 10^4 yrs, the ages for individual sources should be treated with caution since the spindown torque has been observed to vary by more than a factor ~ 4 in the SGRs SGR 1806–20 and SGR 1900+14. The pulse timing properties are summarized in Table 16.2.

Long-term phase-coherent timing of SGRs and AXPs recently became feasible with *RXTE*. Currently several AXPs have continuous timing solutions, with some dating back to 1998 (e.g. Gavriil & Kaspi 2002). In the case of two AXPs (1E 1048.1–5937 [Kaspi et al. 2001]; XTE J1810–197 [Ibrahim et al. 2004]) and two SGRs (SGR 1806–20 and SGR 1900+14 [Woods et al. 2002]) phase-coherent timing is not always possible but has been obtained over stretches of months to years. Major results of this timing effort have been the discoveries of three glitches from two AXPs and strong timing noise detected in both SGRs and the AXP 1E 1048.1–5937.

The occurrence of large glitches is a natural consequence of the magnetar model (Thompson & Duncan 1996) and was even suspected to be the primary source of timing noise in various models of the AXPs (Ussov 1994; Heyl & Hernquist 1999). In 1999, the first glitch from an AXP was ob-

Table 16.2. *Pulse timing properties of the SGRs and AXPs.*

Source	Period (s)	Period Derivative (10^{-11} s s $^{-1}$)	Magnetic Field ^a (10^{14} Gauss)	Spindown Age ^b (10^3 years)	Pulsed Fraction ^c (% rms)
SGR 0526–66	8.0	6.6	7.4	1.9	4.8
SGR 1627–41	6.4?	–	–	–	<10
SGR 1806–20	7.5	8.3–47	7.8	1.4	7.7
SGR 1900+14	5.2	6.1–20	5.7	1.3	10.9
CXOU 010043.1–721134	8.0	–	–	–	10
4U 0142+61	8.7	0.20	1.3	70	3.9
1E 1048.1–5937	6.4	1.3–10	3.9	4.3	62.4
1RXS J170849–400910	11.0	1.9	4.7	9.0	20.5
XTE J1810–197	5.5	1.5	2.9	5.7	42.8
1E 1841–045	11.8	4.2	7.1	4.5	13
AX J1844–0258	7.0	–	–	–	48
1E 2259+586	7.0	0.048	0.60	220	23.4

a – $B_{\text{dipole}} = 3.2 \times 10^{19} \sqrt{P\dot{P}}$ G (the mean surface dipole field)

b – Characteristic age of pulsar spinning down via magnetic braking ($P/2\dot{P}$)

c – $f_{\text{rms}} = \sqrt{\frac{1}{N} \sum_{i=1}^N (r_i - r_{\text{avg}})^2 - e_i^2 / r_{\text{avg}}}$, where N = number of phase bins, r_i is the count rate (2–10 keV) in the i^{th} phase bin, and e_i is the error in the count rate

REFERENCES – (SGR 0526) Kulkarni et al. 2003; (SGR 1627) Woods et al. 1999a; (SGR 1806) Woods et al. 2002; (SGR 1900) Woods et al. 2002; (CXO 0100) Lamb et al. 2003b; (4U 0142) Gavriil & Kaspi 2002; (1E 1048) Kaspi et al. 2001; Gavriil & Kaspi 2004; (RXS 170849) Gavriil & Kaspi 2002; (XTE 1810) Ibrahim et al. 2004; (1E 1841) Gotthelf et al. 2002; (AX 1844) Gotthelf & Vasisht 1998, Torii et al. 1998; (1E 2259) Gavriil & Kaspi 2002

served by *RXTE* in the source 1RXS J170849.0–400910 (Kaspi, Lackey & Chakrabarty 2000). Since that time, another glitch was detected from the same source (Kaspi & Gavriil 2003; Dall’osso et al. 2003) and one glitch was observed in 1E 2259+586 coincident with a burst active episode (Kaspi et al. 2003; Woods et al. 2004). No glitches have been directly observed in the SGRs, although SGR 1900+14 has shown evidence for rapid spin-down at the time of the August 27 flare (see §16.5.4). The magnitude of the angular momentum exchange within the star that one infers for the AXP glitches is more characteristic of Crab-type pulsar glitches than the larger Vela-type

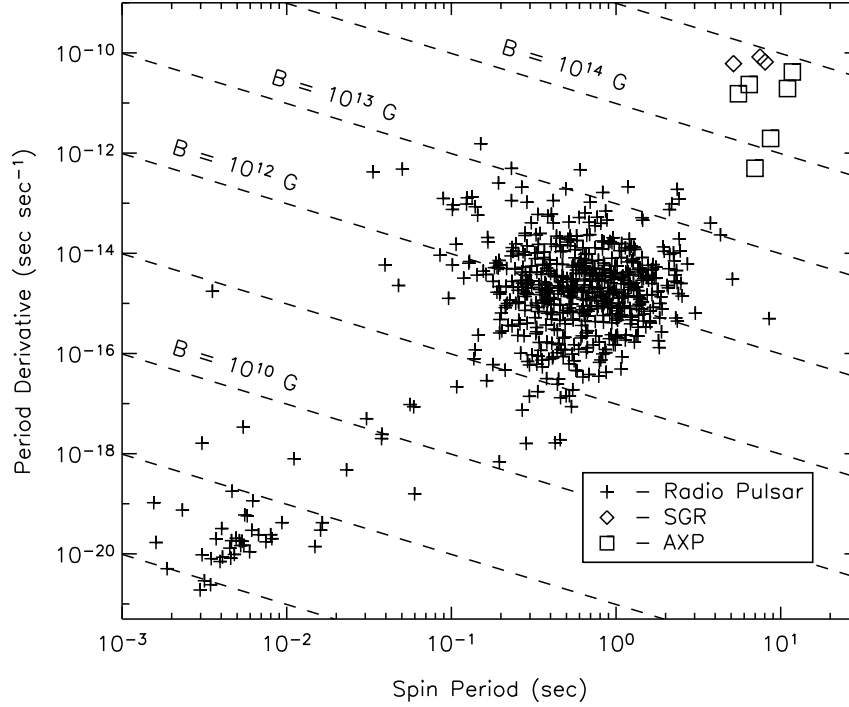


Fig. 16.11. Period versus period derivative for radio pulsars (plus signs), Anomalous X-ray Pulsars (squares), and Soft Gamma Repeaters (diamonds). Contours of constant inferred magnetic field strength are drawn as diagonal dashed lines. Radio pulsar data courtesy of D. Lorimer. AXP and SGR timing data are given in Table 16.2.

glitches, but there are some dissimilarities with radio pulsars glitch behavior (Table 16.3).

The glitch observed from 1E 2259+586 was especially interesting in that it coincided with a SGR-like outburst, and also with changes in the X-ray flux and pulse profile that persisted for months (see §16.5.3). There is evidence for a very long-term component of the post-glitch frequency recovery (consistent with a persistent change in torque) in this glitch, as well as in one of the glitches of 1RXS J170849.0–400910. Overall one observes a great diversity in behavior even within this small sample of glitch events, and more extended monitoring is required to unravel the relationship between glitch behavior and burst activity.

In addition to rapid spin down, all SGRs and AXPs have shown significant timing noise: an irregular drift of the spin frequency superposed on the secular spin down trend. Recent timing solutions have shown that most of

Table 16.3. *Properties of the three glitches observed in two AXPs.*

Source	1RXS J1708–40	1RXS J1708–40	1E 2259+586
$\Delta\nu/\nu^a$	5.5×10^{-7}	1.4×10^{-7}	3.7×10^{-6}
$\Delta\nu_g/\nu$	$> 6.1 \times 10^{-6}$
τ_g (days)	14
$\Delta\nu_d$...	4.1×10^{-6}	$\sim \Delta\nu_g/\nu$
τ_d (days)	...	50	16
$\Delta\dot{\nu}/\dot{\nu}$	-0.010	$< 0.001 $	+0.022
t_{glitch} (MJD TDB)	51444.6	52014.2	52443.1

a – Frequency denoted by ν and frequency derivative by $\dot{\nu}$. The subscript g indicates the frequency growth terms and d indicates decay terms.

REFERENCES – (1RXS 1708) Kaspi & Gavriil 2003; Dall’Osso et al. 2003; (1E 2259) Woods et al. 2004

this noise is not caused by resolved glitches. The existence of timing noise was first noted for the AXPs 1E 2259+586 (e.g. Baykal & Swank 1996) and 1E 1048.1–5937 (e.g. Oosterbroek et al. 1998). Its strength was estimated in four AXPs by Heyl & Hernquist (1999), and was found to be marginally consistent with an extrapolation of the correlation between timing noise strength and braking torque observed in radio pulsars (e.g. Arzoumanian et al. 1994).

In the *RXTE* era, the first direct detection of timing noise was made in SGR 1806–20 (Woods et al. 2000). This SGR is one of the “noisiest” rotators among SGRs and AXPs and has shown a long-term persistent change in torque, along with large stochastic offsets in the X-ray pulse phase on timescales as short as $\sim 10^4$ s (Woods et al. 2002). Although the strength of the timing noise is consistent with some of the “quieter” accreting X-ray pulsars, the shape of the torque power spectrum is more similar to that observed in radio pulsars. Overall, the timing analysis of the AXPs (Kaspi et al. 2001; Gavriil & Kaspi 2002) and one other SGR (Woods et al. 2002) has revealed a broad range of torque variability, with some evidence for a correlation between the strength of the timing noise and the spin-down rate.

16.5 Burst-Induced Variability

It has become evident that burst activity in the SGRs can have a persistent effect on the underlying X-ray source. During the 1998 burst activation of SGR 1900+14, the X-ray counterpart became brighter, its energy spec-

trum was altered, and the pulse shape changed dramatically. Furthermore, the X-ray counterpart to SGR 1627–41 has become progressively dimmer since the one recorded outburst from this SGR in 1998. Finally, the AXP 1E 2259+586 showed a broad array of spectral and temporal changes coincident with its 2002 outburst. We now present some details of the burst-induced variability that is observed in magnetar candidates.

16.5.1 X-ray Afterglows and AXP Outbursts

Extended X-ray afterglow has been detected following four separate bursts from SGR 1900+14. The first such detection followed the giant flare of 1998 August 27 (Woods et al. 2001). One half hour following the flare, the persistent X-ray flux from SGR 1900+14 remained ~ 700 times brighter than the pre-flare level. The X-ray flux decayed over the next 40 days approximately as a power law in time ($F \propto t^{-\alpha}$ with an exponent $\alpha = 0.71$). The blackbody component of the X-ray spectrum was hotter ($kT = 0.94$) one day into the afterglow phase (Woods 2003) than it was before the burst ($kT = 0.5$ keV); but eighteen days later the power-law component of the spectrum was again dominant.

Afterglows have also been detected from SGR 1900+14 following bursts on 1998 August 29 (Ibrahim et al. 2001; Lenters et al. 2003 [Figure 16.12]), 2001 April 18 (Feroci et al. 2003), and 2001 April 28 (Lenters et al. 2003). A power-law decay is also seen in these cases, with a return to the pre-burst flux level between 10^4 and 10^6 s following the burst. Enhanced thermal emission is typical, with temperatures as high as ~ 4 keV (corresponding to a hot spot covering ~ 1 percent of the neutron star surface). In fact, the afterglow of the 2001 April 28 burst involved only enhanced thermal emission. Within this small sample of afterglows from SGR 1900+14, the 2 – 10 keV afterglow energy is about 2% of the 25 – 100 keV burst energy (Lenters et al. 2003).

Resolved observations of individual SGR burst afterglows are still rare, because they require pointed X-ray observations coincident with a burst (or very soon thereafter). It is much easier to observe the collective effect of SGR burst activity on the persistent X-ray flux, as is seen in the case of SGR 1900+14 (Figure 16.13).

The detection of X-ray bursts (Kaspi et al. 2003) from the AXP 1E 2259+586 was the fortunate result of a long-term monitoring campaign by *RXTE*. The X-ray flux of this source increased by at least a factor ~ 20 on 2002 June 18 (Woods et al. 2004), during which more than 80 SGR-like bursts were emitted (Gavriil et al. 2004). This first component of the flux decay was

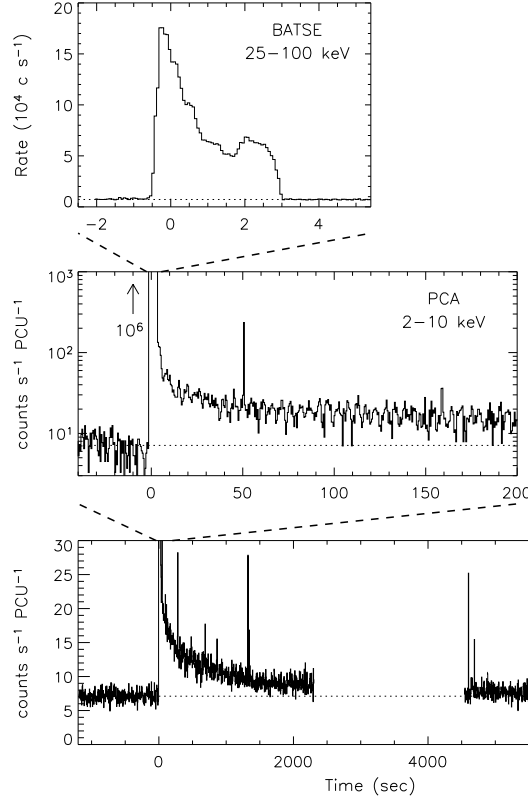


Fig. 16.12. The time history of the August 29th burst and its afterglow. *Top* - The BATSE light curve showing the sharp rise and fall of the burst. *Middle* - The PCA light curve including the burst (off-scale) and the early portions of the afterglow ($T+3$ s). There is a sharp discontinuity in the energy spectrum when the high-luminosity burst emission terminates at 3 s (Ibrahim et al. 2001) indicating the transition from the burst to the afterglow. Note the clear 5.16 s pulsations in the light curve. *Bottom* - The PCA light curve over a longer time interval showing the gradual decay of the afterglow. The spectral evolution during the afterglow is presented in Ibrahim et al. (2001) and Lenters et al. (2003). The horizontal dotted lines in all panels represent the background level.

spectrally hard, contained all of the observed burst activity, and involved only ~ 1 percent of the neutron star surface. It decayed within ~ 1 day, and was followed by a much more gradual flux decay over the following year. This more extended X-ray brightening involved a significant fraction of the warm stellar surface, but only a modest spectral hardening. No bright burst (similar to the intermediate bursts of the SGRs) appears to have preceded this activity.

The longer term flux variability of the SGR and AXP sources is still un-

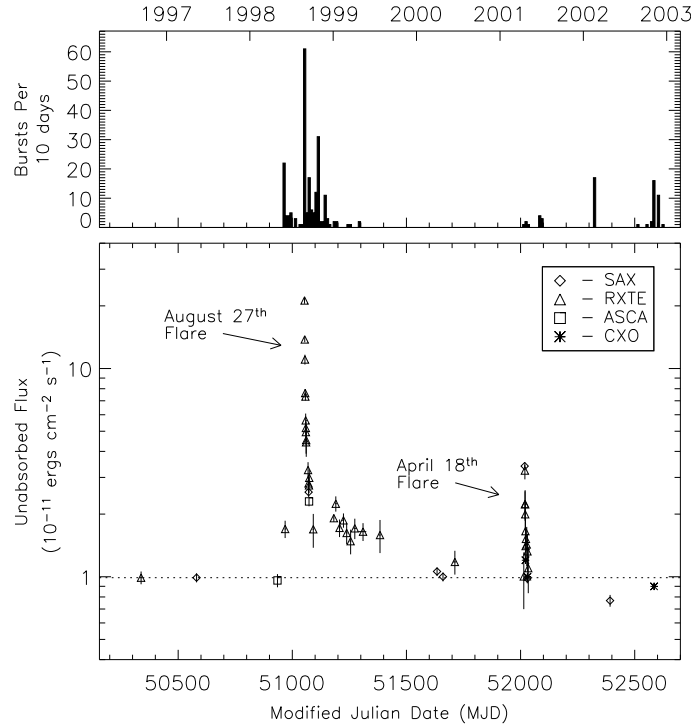


Fig. 16.13. *Top panel* – Burst rate history of SGR 1900+14 as observed with BATSE and the IPN. *Bottom panel* – Persistent/Pulsed flux history of SGR 1900+14 covering 5.5 years. The vertical scale is unabsorbed 2–10 keV flux. The pulsed fraction is assumed constant to convert pulsed flux to phase-averaged flux (see Woods et al. 2001 for details). The dotted line marks the nominal quiescent flux level of this SGR. Note the strong correlation between the burst activity and the flux enhancements.

clear. Some sources (such as the AXPs 1E 2259+586, 1E 1048.1–5937, and 4U 0142+61) have remained X-ray bright for two-three decades. A previous X-ray brightening of 1E 2259+586 detected 10 years earlier by Ginga (Iwasawa, Koyama & Halpern 1992) allows one to deduce that at least $\sim 10\%$ of the X-ray output of this source is released in transient events. A steady decrease in X-ray flux was also observed in SGR 1627–41 after its outburst in June/July 1998, but this was followed by a sharper drop a few years later (Kouveliotou et al. 2003). The X-ray flux of this source has appeared to level off at a value ($\sim 4 \times 10^{33} \text{ ergs s}^{-1}$) consistent with the low state levels seen in at least two other sources. It is possible that magnetar candidates become increasingly intermittent X-ray sources as they age; alternatively, some intermittent sources may have weaker magnetic fields. There is, nonetheless,

clear evidence for both short-term and long-term flux variability associated with X-ray outbursts.

16.5.2 Transient Counterparts at other Wavelengths

The only recorded radio emission from a magnetar candidate was associated with the 1998 August 27 giant flare of SGR 1900+14 (Frail, Kulkarni & Bloom 1999). No radio detection was made before or since; but a faint transient persisted for 2 weeks following the X-ray flare with a spectral index of -0.74 ± 0.15 . No similar radio detections have been made following other SGR outbursts (all of which were much less energetic than the August 27 flare and probably involved a much weaker particle outflow).

Optical and/or infrared (IR) counterparts have been discovered in four (possibly five) magnetar candidates (see §16.6.4). The IR flux of the AXP 1E 2259+586 increased following its 2002 June outburst (Kaspi et al. 2003). A week after the X-ray burst activity, the *K*-band flux was 3.4 times higher than measured two years earlier; it had returned near its pre-outburst level after ~ 40 days (Israel et al. 2003a).

Automated telescopes such as ROTSE have observed SGRs during burst active periods (Akerlof et al. 2000). On a few occasions, optical images have been acquired shortly after bright bursts from SGR 1900+14. No transient optical emission has been seen down to limiting V-band magnitudes of ~ 12.5 – 15.5 . However, the visual extinction toward SGR 1900+14 is extremely high and so these limits are not constraining. Followup observations of SGR bursts particularly with robotic IR cameras with fast photometric capabilities, could provide interesting constraints on the burst mechanism.

16.5.3 Changes in X-ray Pulse Shape and Pulsed Fraction

Changes in the X-ray pulse profile have been observed in magnetar candidates during periods of intense burst activity. The most profound changes in pulse properties have been observed in SGR 1900+14. In particular, at the time of the giant flare of 1998 August 27, the pulse profile of the persistent emission changed dramatically from a complex, multi-peaked morphology to a simple, nearly sinusoidal morphology (Figure 16.14). The change in pulse shape has persisted even years after the post-flare afterglow faded away (Gögüş et al. 2002). The effectively permanent change in pulse shape observed in SGR 1900+14 argues for a magnetic field reconfiguration at the time of the giant flare (Woods et al. 2001). A similar simplification of the pulse shape was observed – at a much higher flux level – over the last few

minutes of the August 27 flare (Figure 16.14). This change in pulse profile was smooth and gradual; indeed, the flux decline was consistent with cooling of a magnetically confined plasma (Feroici et al. 2001). Thus, the magnetic field reconfiguration may well have been concentrated in the initial impulsive phase of the flare.

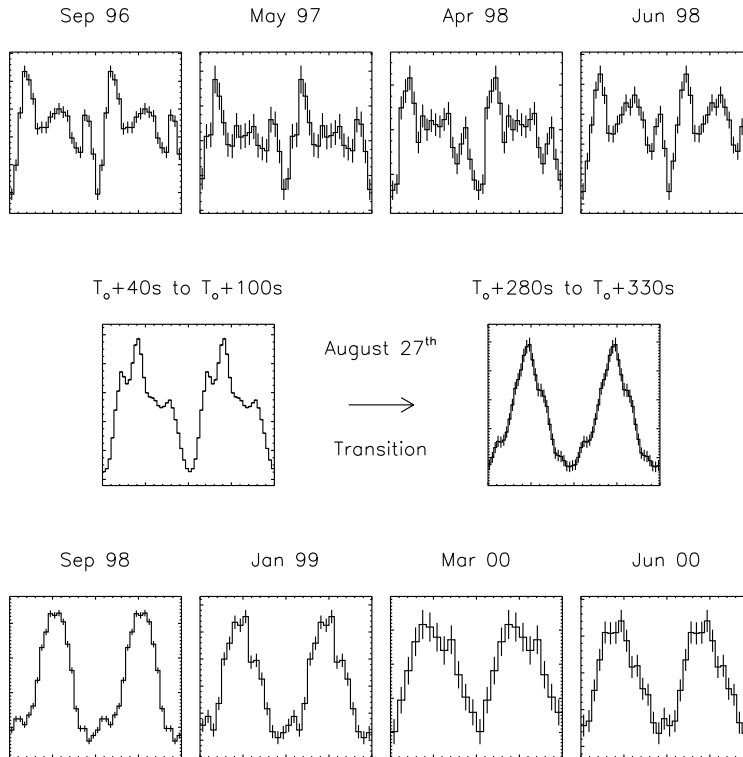


Fig. 16.14. Evolution of the pulse profile of SGR 1900+14 from 1996 September through 2000 April (Woods et al. 2001). All panels display two pulse cycles and the vertical axes are count rates with arbitrary units. The two middle panels were selected from *Ulysses* data (25–150 keV) of the August 27th flare. Times over which the *Ulysses* data were folded are given relative to the onset of the flare (T_0). The top and bottom rows are integrated over the energy range 2–10 keV. From top-to-bottom, left-to-right, the data were recorded with the *RXTE*, *BeppoSAX*, *ASCA*, *RXTE*, *RXTE*, *RXTE*, *BeppoSAX*, and *RXTE*.

A significant change in pulse shape was also observed in SGR 1806–20 between 1996 and 2001 (Gögüş et al. 2002). The change was not as dramatic as in SGR 1900+14; but the source also emitted far less energy in X-ray bursts than was released in the August 27 flare. More subtle changes in pulse shape were also observed in SGR 1900+14 between 1999 and 2001, when it

underwent intermittent burst activity. During the 2002 June 18 outburst of 1E 2259+586, the pulse profile evolved rapidly showing large changes in the relative amplitudes of the two peaks (Kaspi et al. 2003; Woods et al. 2004). Some residual change has persisted at least until one year after the burst activity. In sum, the connection between X-ray outbursts and pulse shape changes can be subtle, and frequent monitoring of magnetar candidates will be required to understand it better.

Large changes in pulsed fraction have been observed in magnetar candidates during periods of burst activity. During burst afterglows of SGR 1900+14, the rms (2–10 keV) pulsed fraction has been observed to rise to $\sim 20\text{--}30\%$ from its quiescent value of $\sim 11\%$ (Lenters et al. 2003). Intriguingly, the enhanced pulsations remain in phase with the pre-burst pulsations in at least two bursts. This indicates a direct correlation between the source of the pulsed X-ray emission and the active burst region.

A pulsed fraction change was also observed in 1E 2259+586 during its 2002 June outburst (Woods et al. 2004). During the *RXTE* observation where the burst activity was observed, the pulsed fraction (2–10 keV) actually *decreased* to $\sim 15\%$ from the pre-outburst level of 23.4%. The pulsed fraction recovered to $\sim 23.4\%$ within ~ 6 days of the outburst, much more rapidly than the pulse shape recovered.

16.5.4 Connection with Timing Anomalies

X-ray burst activity appears to have a variety of effects on the spin behavior of magnetar candidates. A comparison of the spin evolution of SGR 1900+14 before and after the August 27 flare showed that the source underwent a transient spindown within an 80 day window that bracketed the flare (Woods et al. 1999c). The decrease in spin frequency, by one part in 10^4 , was opposite in sign to pulsar glitches. A comparison of the pulse timing during and after the flare indicate that the change in frequency occurred within several hours of the flare (Palmer 2002). The amplitude of the spindown is consistent with an enhanced magnetic torque due to a relativistic outflow of particles (Thompson & Blaes 1998; Frail et al. 1999; Thompson et al. 2000) if the dipole field of the star is $\sim 10^{15}$ G.

Only the giant flare from SGR 1900+14 has shown direct evidence for burst-induced spindown. This SGR suffered another timing anomaly at the time of the 2001 April 18 flare, but sparse data coverage did not allow for an unambiguous determination of its nature (Woods et al. 2003). More than 5 years of timing and burst data for each SGR have revealed longer-term increases in braking torque, of similar magnitudes, that are not however

synchronized with burst activity. (Indeed the output in X-ray bursts from SGR 1806–20 was much smaller than from SGR 1900+14 over this time interval.) There is, nonetheless, some tentative evidence for a causal relation between burst activity and torque variability, in that the most burst-active magnetar candidates are also those which show the strongest timing noise.

A timing anomaly of a different type, the glitch of 1E 2259+586 (§16.4), coincided with the 2002 June X-ray outburst (Kaspi et al. 2003; Woods et al. 2004). Since the beginning of the X-ray activity was not observed, it was not possible to determine whether it preceded, overlapped, or followed the onset of the glitch. Nonetheless, the change in rotational energy associated with the glitch was much smaller than the energy released in the X-ray transient, suggesting that the trigger involved some other agent (e.g. the release of magnetic stresses).

In the case of the SGRs, glitches of the magnitude seen in 1E 2259+586 cannot generally be excluded: the timing ephemerides preceding X-ray outbursts are less accurate for these sources. However, X-ray transients associated with glitches of other AXP sources are easier to constrain. No burst emission was seen near the time of either of the two glitches observed in 1RXS J170849.0–400910 (Kaspi & Gavriil 2003). A ~ 1 day hard-spectrum transient, such as was observed from 1E 2259+586, could easily have been missed. However, the 1E 2259+586 outburst also showed a sustained X-ray afterglow lasting months and a pulse profile change for a somewhat shorter time interval (Woods et al. 2004). The regular monitoring of 1RXS J170849.0–400910 would have been sensitive to changes of this magnitude. Continued phase-coherent timing of these objects is needed to determine the extent to which glitches are accompanied by burst activity.

16.6 Locations, SNR Associations, and Counterparts

A multi-wavelength approach has always proven fruitful for understanding enigmatic astrophysical objects. The SGRs and AXPs are no exception to this rule. Precise determinations of their X-ray locations have allowed follow-up observations at radio and optical/IR wavelengths. We now discuss the results of this collective effort to study the magnetar candidates.

16.6.1 X-ray Localizations

Precise, sub-arcsecond X-ray locations have now been obtained for nearly all magnetar candidates (Table 16.4). In the case of the AXPs, which are discovered as persistent X-ray point sources, these localizations have involved

a refinement of previous measurements. But, for the SGRs, the most precise locations were obtained up to the mid-1990's through triangulation of burst emissions using the Interplanetary Network (IPN). Persistent X-ray counterparts have only been detected since then.

Table 16.4. *The X-ray positions, reported associations, and the inferred distances of the SGRs and AXPs.*

Source	Right Ascension ^b (J2000)	Declination (J2000)	Associated SNR/Cluster	Distance (kpc)	Galactic Scale Height (pc)
SGR 0526–66	05 ^h 26 ^m 00.89 ^s	–66° 04′ 36.3″	N49/cluster?	50	n/a
SGR 1627–41	16 ^h 35 ^m 51.84 ^s	–47° 35′ 23.3″	...	11	–21
SGR 1801–23 ^b	18 ^h 00 ^m 59 ^s	–22° 56′ 50″	...	~10	...
SGR 1806–20	18 ^h 08 ^m 39.32 ^s	–20° 24′ 39.5″	cluster	15	–63
SGR 1900+14	19 ^h 07 ^m 14.33 ^s	+09° 19′ 20.1″	cluster	15	+200
CXOU 010043.1–721134	01 ^h 00 ^m 43.14 ^s	–72° 11′ 33.8″	...	57	n/a
4U 0142+61	01 ^h 46 ^m 22.42 ^s	+61° 45′ 02.8″	...	3	–20
1E 1048.1–5937	10 ^h 50 ^m 07.14 ^s	–59° 53′ 21.4″	...	3	–27
1RXS J170849–400910	17 ^h 08 ^m 46.87 ^s	–40° 08′ 52.4″	...	5	+3
XTE J1810–197	18 ^h 09 ^m 51.08 ^s	–19° 43′ 51.7″	...	~10	...
1E 1841–045	18 ^h 41 ^m 19.34 ^s	–04° 56′ 11.2″	G27.4+0.0	7	–1
AX J1844–0258 ^c	18 ^h 44 ^m 53 ^s	–02° 56′ 40″	G29.6+0.1	~10	+20
1E 2259+586	23 ^h 01 ^m 08.30 ^s	+58° 52′ 44.5″	G109.1–1.0	3	–52

a – All positions accurate to $<1''$ unless otherwise noted

b – Only a very crude IPN location (~ 80 arcmin² area) exists for this SGR

c – The positional accuracy for this AXP is a 20'' radius circle

REFERENCES – (SGR 0526) Kulkarni et al. 2003; Klose et al. 2004; (SGR 1627) Wachter et al. 2004; Corbel et al. 1999; (SGR 1801) Cline et al. 2000; (SGR 1806) Kaplan et al. 2001; Fuchs et al. 1999; Corbel & Eikenberry 2004; (SGR 1900) Frail et al. 1999; Vrba et al. 2000; (CXO 0100) Lamb et al. 2002; (4U 0142) Patel et al. 2003; Hulleman, van Kerkwijk & Kulkarni 2004; (1E 1048) Wang & Chakrabarty 2002; (RXS 170849) Israel et al. 2003b; (XTE 1810) Israel et al. 2004; (1E 1841) Wachter et al. 2004; Vasisht & Gotthelf 1997; (AX 1844) Vasisht et al. 2000; Gaensler et al. 1999; (1E 2259) Patel et al. 2001; Kothes, Uyaniker & Aylin 2002

The distances to the SGRs and AXPs have been estimated in several several different ways, with widely varying degrees of precision (Table 16.4). One SGR (SGR 0526–66) and one AXP candidate (CXOU J0110043.1–721134) are located in the Large and Small Magellanic Clouds, respectively, and have well-determined distances. Two AXPs (1E 2259+586 and 1E 1841–045) are

positioned close to the centers of SNR and are, very likely, physically associated (see §16.6.2). Both SGR 1806–20 and SGR 1900+14 may be associated with massive star clusters (see §16.6.4), each of which has an estimated distance. Most other distances rely on the measurement of interstellar absorption from X-ray spectra, and the intervening distribution of molecular clouds. A more complete discussion of the distance uncertainties is given in Özel et al. (2001).

All except two of the magnetar candidates are located within our Galaxy, and are positioned close to the Galactic plane. Their estimated heights above (or below) the Galactic plane for these sources are given in Table 16.4. The small rms scale height ($z_{\text{rms}} \simeq 70$ pc) implies a young source population. This is consistent with the young ages inferred from the spin parameters (Table 16.2) and the SNR associations.

16.6.2 SNR Associations

Supernova remnants are the glowing relics of massive explosions produced during the formation of some neutron stars. The surface brightness of a SNR depends upon its age and the density of the local inter-stellar medium. Because of dimming and observational selection (see e.g. Gaensler & Johnston 1995), not every SNR contains a young pulsar. Likewise, young pulsars are not always found in SNRs. In fact, only one third of young ($<10^5$ yr) pulsars are expected to be found positionally coincident with their associated SNRs, which is entirely consistent with the observed fraction.

As shown by Gaensler et al. (2001), the situation is similar for the AXPs and SGRs as a group. Of the 10 confirmed magnetar candidates, only 2 have solid SNR associations (1E 2259+586 with CTB 109 [Gregory & Fahlman 1980] and 1E 1841–045 with Kes 73 [Vasisht & Gotthelf 1997]). The AXP candidate AX J1845–0258 has a solid association with the SNR G29.6+0.1 (Gaensler et al. 1999). Assuming that the SGR/AXP kick velocities incurred at birth are similar to those of radio pulsars, and given the space density of SNRs in the LMC, the association of SGR 0526–66 with the SNR N49 (Cline et al. 1982) was shown to be less secure than previously thought: the probability of a chance alignment is about 0.5% (Gaensler et al. 2001). These authors argued that other SGR/SNR and AXP/SNR associations reported in the literature were unconvincing, or likely to be chance superpositions.

The ages of the remnants associated with the magnetar candidates are $\sim 10^4$ yr, consistent with other age estimates for most of these objects. Other than containing a magnetar candidate, there is nothing unusual about these two SNRs relative to those of comparable age which are associated with

radio pulsars. Note also that the young characteristic age of SGR 1900+14 ($\sim 10^3$ yrs) would make the absence of a SNR counterpart surprising, unless its true age were significantly larger (Thompson et al. 2000).

16.6.3 Radio Limits

Despite deep, sensitive radio observations of most magnetar candidates, no persistent radio emission has been detected from any SGR or AXP. The only recorded radio detection of a magnetar candidate was a transient outburst seen from SGR 1900+14 in the days following the 1998 August 27 flare (see §16.5.2). Pulsed emission from this SGR in 1998 near the X-ray pulse period (5.16 s) was reported using 100 MHz data taken with the BSA (Shitov 1999), but the radio ephemeris disagreed significantly with the X-ray ephemeris (Woods et al. 1999c).

The non-detections of magnetar candidates at radio frequencies does not necessarily mean that they are very different from standard pulsars in their radio properties (Gaensler et al. 2001). Most pulsars are expected to have fluxes below the current limits for the AXPs. Long-period pulsars tend to have narrower beams (<1 deg), effectively reducing the chances that their beams will cross our line-of-sight. Given the small number of observed SGRs and AXPs, it is not surprising that none are detected.

The Parkes Multi-Beam Survey has revealed a handful of radio pulsars with magnetar strength fields as inferred from their spin parameters (Camilo et al. 2000; McLaughlin et al. 2003). These pulsars have X-ray luminosities much lower than their AXP/SGR counterparts (Pivovarov, Kaspi & Camilo 2000), in spite of their similar dipole field strengths. This result has led Pivovarov et al. and others (Camilo et al. 2000; McLaughlin et al. 2003) to conclude that membership as an AXP (or SGR) requires more than just a strong dipole magnetic field. Nonetheless, it would not be surprising to observe the transition of a high-field radio pulsar to a brighter X-ray state, given the realization that some magnetar candidates can enter X-ray low states for extended periods of time.

16.6.4 Optical and IR Counterparts

The first optical detection of a magnetar candidate, the AXP 4U 0142+61, was made by Hulleman et al. (2000). They discovered an object with unusual colors spatially coincident with the X-ray position of the AXP. The broadband spectrum of 4U 0142+61 is shown in Figure 16.15. Since this initial discovery, at least four other optical/IR counterparts with similar charac-

teristics have been discovered for other AXPs (and possibly one SGR). The optical/IR properties of the magnetar candidates are given in Table 16.5. See also Hulleman, van Kerkwijk & Kulkarni (2004) for a table of empirically estimated magnitudes of those sources not yet discovered.

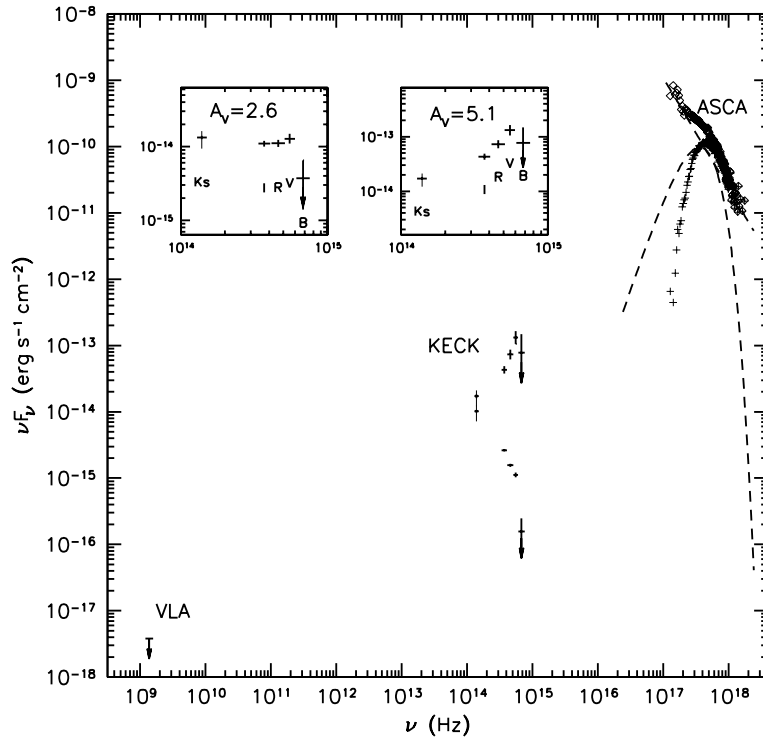


Fig. 16.15. Energy distribution for 4U 0142+61 (Hulleman et al. 2004). At low frequencies (10^{14} – 10^{15} Hz), the points marked V, R, I, K_s indicate the observed V, R, I, and K_s-band fluxes. The vertical error bars reflect the uncertainties, while the horizontal ones indicate the filter bandwidths. The set of points above the measurements indicate dereddened fluxes for $A_V = 5.4$, as inferred from the X-ray column density. At high frequencies (10^{17} – 10^{18} Hz), the crosses show the incident X-ray spectrum as inferred from ASCA measurements. The diamonds show the spectrum after correction for interstellar absorption, and the two thick dashed curves show the two components used in the fit. Figure courtesy of M. van Kerkwijk and F. Hulleman.

The discovery of optical/IR counterparts to magnetar candidates has placed valuable new constraints on their nature. Fast photometry of 4U 0142+61 revealed optical (*R* band) pulsations with a high pulsed fraction ($\sim 27\%$ peak-to-peak) at the spin frequency of the neutron star (Kern & Martin 2002). The pulsed fraction of the optical pulsations is comparable to or greater than the pulsed fraction at X-ray energies.

Table 16.5. *Optical and IR magnitudes of SGRs and AXPs.*

Source	V	R	I	J	H	K	K _s
SGR 0526–66	>27.1	...	>25
SGR 1627–41	>21.5	>19.5	...	>20.0
SGR 1806–20 ^b	>21	>20.5	18.6	...
SGR 1900+14	>22.8	>20.8
CXOU 010043.1–721134
4U 0142+61	25.6	25.0	23.8	19.6	20.1
1E 1048.1–5937 ^a	...	>24.8	26.2	21.7	20.8	...	19.4–21.3
1RXS J170849–400910 ^b	20.9	18.6	...	18.3
XTE J1810–197	>24.3	...	22.0	...	20.8
1E 1841–045 ^b	...	>23	19.4
AX J1844–0258
1E 2259+586 ^a	...	>26.4	>25.6	>23.8	20.4–21.7

a – Has shown variability in the infrared

b – Candidate counterpart

REFERENCES – (SGR 0526) Kaplan et al. 2001; (SGR 1627) Wachter et al. 2004; (SGR 1806) Eikenberry et al. 2001; (SGR 1900) Kaplan et al. 2002; (CXO 0100) Lamb et al. 2002; (4U 0142) Hulleman et al. 2000, 2004; (1E 1048) Wang & Chakrabarty 2002; Israel et al. 2002; Durant, van Kerkwijk & Hulleman 2003; (RXS 170849) Israel et al. 2003b; (XTE 1810) Israel et al. 2004; (1E 1841) Wachter et al. 2004, Mereghetti et al. 2001; (1E 2259) Hulleman et al. 2001; Kaspi et al. 2003; Israel et al. 2003a

Monitoring of the optical/IR counterparts of the AXPs has shown that the IR fluxes of the AXPs vary with time and burst activity (§16.5.2). If the IR flux is an indicator of burst emission in AXPs (e.g. 1E 2259+586 in 2002 June), then IR flux variability seen in 1E 1048.1–5937 (Israel et al. 2002) and 4U 0142+61 (Hulleman, van Kerkwijk & Kulkarni 2004) could indicate the presence of undetected bursts. Clearly, continued monitoring of magnetar candidates is required to confirm some of these early findings.

Deep IR observations of the fields of two SGRs have revealed the presence of massive star clusters in which the SGRs are possibly embedded. Fuchs et al. (1999) found that SGR 1806–20 was positionally coincident with a cluster of massive stars at a distance ~ 15 kpc. Indeed, a very luminous star is located close to SGR 1806–20 (van Kerkwijk et al. 1995), but is not positionally coincident with it (Hurley et al. 1999d). Similarly, Vrba et al. (2000) found a cluster of massive stars at a distance ~ 15 kpc surrounding SGR 1900+14. Follow-up IR observations of SGR 1806–20

have revealed two IR sources consistent with the X-ray position of the SGR (Eikenberry et al. 2001), although the ratio of optical to X-ray flux is anomalously large for either optical source, thus neither are likely the counterparts to SGR 1806–20. Analysis of the other members of this cluster have shown that this particular cluster contains some of the most massive stars in our Galaxy, perhaps even the most luminous star in our Galaxy (Eikenberry et al. 2001). These findings suggest that these two SGRs may have very massive progenitors.

Finally, one other avenue open to pursue in optical/IR studies of magnetar candidates is the measurement of proper motion. Hulleman et al. (2000) have already placed a 2σ upper limit of $0.03 \text{ arcsec yr}^{-1}$ to the proper motion of 4U 0142+61. Some models of magnetar formation (e.g. Duncan & Thompson 1992) suggest high kick velocities incurred at birth. The precise astrometry available with optical/IR observations will allow tighter constraints on the proper motions of the AXPs and SGRs, and shed further light on the physical connection of these sources to nearby SNR.

16.7 Magnetar Model

We will organize our discussion of the magnetar model around its predictions, the extent to which they have been verified or falsified, and outline areas in which further advancement of theory is needed to make quantitative comparisons with data. The basic idea of the model is that the variable X-ray emission – the bursts lasting up to ~ 1000 s and the transient changes in persistent emission observed up to ~ 1 yr – are powered by the decay of the star’s magnetic field. A rms field exceeding $\sim 10^{15}$ G is needed to supply an output of $10^{35} \text{ erg s}^{-1}$ extending over 10^4 yrs.

The AXPs as a group are systematically much brighter thermal X-ray sources than radio pulsars of the same characteristic age. The evidence for repeated bulk heating of the crust, and the relative brightness of the X-ray emission, has bolstered the suggestion that magnetic field decay is the main energy source for that emission. That conclusion is most secure in those AXP sources which show large transient swings in X-ray brightness over a period of years. The non-thermal X-ray emission of the SGRs cannot be powered primarily by cooling or by spindown.

In the magnetar model, this enhanced X-ray emission results from four effects (Thompson & Duncan 1996; Heyl & Kulkarni 1998; Colpi, Geppert, & Page 2000; Thompson, Lyutikov, & Kulkarni 2002; Kouveliotou et al. 2003; Arras, Cumming, & Thompson 2004): i) internal heating by field decay; ii) a modest increase in the thermal transmissivity of the envelope due to

the strong surface magnetic field (van Riper 1988, Heyl & Hernquist 1998; Potekhin & Yakovlev 2001); iii) a delay in the transition to core neutron superfluidity caused by magnetic heating (after this transition, a neutron star undergoes a significant drop in surface X-ray flux: Yakovlev et al. 2001); and iv) surface heating, and cyclotron scattering of thermal surface emission, by charged particles which supply electric currents outside the star. Microscopic transport of the magnetic field in neutron star interiors has been considered in detail by Haensel, Urpin, & Yakovlev (1990), Goldreich & Reisenegger (1992), and Pethick (1992). Sweeping of magnetic fluxoids out of a superconducting core by the interaction with the superfluid vortices has been considered as a mechanism of magnetic field decay in radio pulsars (Ruderman, Zhu, & Chen 1998). It may, however, be suppressed if the field is stronger than $\sim 10^{15}$ G and the fluxoids are tightly bunched.

The behavior of the SGRs and AXPs has not been observed over baselines longer than ~ 20 – 30 yrs. Some AXPs such as 1E 2259+586 and 4U 0142+61 have sustained bright ($\sim 10^{35}$ erg s $^{-1}$) thermal X-ray emission over this period of time, which is comparable to or longer than the thermal conduction time across the crust (Gnedin et al. 2001). Their duty cycle as bright X-ray sources is presently unknown.

16.7.1 Mechanism for Magnetar Bursts

Both the short and the long outbursts of magnetars are hypothesized to arise from the direct injection of energy into the magnetosphere, through a rearrangement of the magnetic field and the formation and dissipation of strong localized currents. Magnetar flares are distinguished from Solar flares in two key respects (Thompson & Duncan 1995): the magnetic field is anchored in a rigid medium (the lower crust) which has some finite shear strength; and the energy density in the magnetic field is high enough that rapid thermalization of energized charged particles can be expected. (In the short SGR bursts, the rate of release of energy is not rapid enough to effect complete thermalization and drive the photon chemical potential to zero, but it is at the onset of the giant flares; Thompson & Duncan 2001.)

The crust provides a plausible site for the initial loss of equilibrium that triggers an outburst. For example, the relaxation behavior observed over a period of weeks in SGR 1806-20 (Palmer 1999) suggests that the release of energy in successive short SGR bursts is limited by inertial and frictional forces. In addition, bursts similar to short SGR bursts are observed to begin at least two larger events: the August 27 and August 29 flares of SGR 1900+14. The duration of the short bursts is comparable to the time

for a torsional deformation to propagate vertically across the crust in a $\sim 10^{14}$ G poloidal magnetic field. The ability of the interior of the star to store much stronger toroidal magnetic fields than the exterior provides a hint that the ensuing burst is driven primarily by a loss of equilibrium in the crust, rather than by reconnection and simplification of non-potential magnetic fields outside the star. Nonetheless, it is likely that both effects will occur in concert, given the magnitude of the energies released.

The initial spikes of the giant flares have been associated with expanding fireballs composed of e^\pm pairs and non-thermal gamma-rays (Paczyński 1992), and the pulsating tails with thermalized energy which remains confined close to the neutron star by its magnetic field (Thompson & Duncan 1995). In the spikes, the combination of rapid (< 0.01 s) variability with a hard non-thermal spectrum points to a low baryon contamination. The argument that most of the flare energy is deposited in the first second comes from i) the near coincidence between the energy of the initial spike and the energy radiated over the remaining ~ 300 s of the burst; and ii) the smooth adiabatic simplification of the pulse profile in the tail of the 27 August 1998 flare, which shows no evidence for secondary impulsive injections of energy that would be associated with a continuing substantial reorientation of the magnetic field. The lower bound on the magnetic moment implied by the confinement of $\sim 10^{44}$ ergs is $BR_{NS}^3 \simeq 10^{14}$ G (Thompson & Duncan 2001).

Large-scale deformations of the crust are constrained by its high hydrostatic pressure, but varying implications have been drawn for its elastic response to evolving magnetic stresses. One possibility is that the crust develops a dense network of small-scale (but macroscopic) dislocations, and that the resulting fast ohmic heating of the uppermost layers of the star is what powers the extended afterglow observed following SGR flares (Lyubarsky, Eichler, & Thompson 2002). Alternatively Jones (2003) and Lyutikov (2003) raise the possibility that the response of the crust may be more gradual and purely plastic, which would force the main source of energy for an X-ray flare into the magnetosphere. Evidence that the shear deformations of the crust are spatially concentrated comes from the observation of hard thermal X-ray emission – covering $\sim 1\%$ of the surface area of the star – right after the August 29 flare of SGR 1900+14 (Ibrahim et al. 2001) and during the transient brightening of 1E 2259+586 (Woods et al. 2004).

16.7.2 Burst Spectral Evolution and Afterglow

A trapped thermal fireball (in which the photons have a Planckian distribution at a temperature ~ 1 MeV) is very optically thick to scattering, given

the high density of electron-positron pairs. It releases energy through the contraction of its cool surface – in contrast to the cooling of a material body of fixed surface area. Thus, the X-ray flux is predicted to drop rapidly toward the end of a flare, when the external fireball evaporates (Thompson & Duncan 1995). A simple model of a contracting spherical surface, bounding a fireball with a modest temperature gradient, provides an excellent fit to the 27 August 1998 flare (Feroci et al. 2001).

The temperature of the fireball surface is also buffered by a quantum electrodynamic effect: X-ray photons propagating through intense magnetic fields are able to split in two or merge together (Adler 1971). The rate of splitting grows rapidly with photon frequency, but loses its dependence on magnetic field strength when $B \gg B_{QED} = 4.4 \times 10^{13}$ G (Thompson & Duncan 1992). Energy and momentum are both conserved in this process, with the consequence that only one polarization mode can split. As a result, splitting freezes out below a characteristic black body temperature of ~ 12 keV in super-QED magnetic fields (Thompson & Duncan 1995). This is, very nearly, the temperature observed during an extended period of flux decline in the pulsating tail of the 27 August 1998 flare (Feroci et al. 2001). In some geometries, double Compton scattering can also be a significant source of photon seeds near the scattering photosphere (Lyubarsky 2002).

The rate of radiative conduction through an electron gas is greatly increased by the presence of a strong magnetic field, which suppresses the opacity of the extraordinary polarization mode (Sil’antev & Iakovlev 1980; Lyubarskii 1987). Thus, the high luminosities of the intermediate flares, and the pulsating tails of the giant flares, also point to the presence of $10^{14} - 10^{15}$ G magnetic fields (Paczyński 1992). This effect can, however, be suppressed by mode exchange near the stellar surface (Miller 1995), and probably requires a confining magnetic field (Thompson & Duncan 1995).

One clear prediction of the trapped fireball model is that ~ 1 percent of the trapped energy will be conducted into the surface of the neutron star over the duration of the fireball phase (Thompson & Duncan 1995). This energy can explain the prompt afterglow observed immediately following the intermediate burst on 29 August 1998 (Ibrahim et al. 2001), but heat conducted into the crust cannot supply afterglow longer than $\sim 10^4$ s following the burst. The relative importance of such conductive heating for the observed afterglow – as compared with direct bulk heating and continuing relaxation of currents outside the star – is not well understood.

Searches for X-ray lines during SGR bursts are potentially diagnostic of the burst mechanism and the strength of the magnetic field. Short, low-energy SGR bursts are probably highly localized on the neutron star surface.

The magnetosphere is probably at a higher temperature than the surface during a burst, and so proton cyclotron features may be seen in emission in the keV range (if the surface magnetic field is $\sim 10^{14} - 10^{15}$ G).

16.7.3 *Electrodynamics*

Highly non-thermal persistent X-ray emission is observed in the actively bursting SGR sources, and from it one infers the presence of magnetospheric currents much stronger than the rotationally-driven Goldreich-Julian current. Although the spindown power in SGRs 1806-20 and 1900+14 peaks at values approaching the X-ray luminosity during their periods of most extreme spindown torque, there is no correlation between the two. To power the X-ray emission, the energy that must be dissipated per Goldreich-Julian particle on the open field lines exceeds $\sim 10^8$ MeV. By contrast, if the flux of particles close to the stellar surface is normalized to $cB_{\text{NS}}/4\pi eR_{\text{NS}}$, then the energy dissipated per particle need not exceed ~ 100 MeV (e.g. the binding energy of an ion to the star).

The persistent changes in X-ray pulse profile observed following SGR bursts could be caused by a change in the emission pattern; or by a change in the distribution of particles which rescatter the X-rays higher in the magnetosphere (e.g. at ~ 10 neutron star radii where the cyclotron resonance of the electrons is in the keV range). For example, in a magnetosphere threaded by persistent electric currents, the optical depth at the cyclotron resonance of the current-carrying charges is of the order of unity over a continuous range of frequencies (if the poloidal magnetic field is twisted through ~ 1 radian; Thompson et al. 2002). In such a situation, an X-ray photon will undergo a significant shift in frequency as it escapes the magnetosphere.

A non-thermal component of the X-ray spectrum is not always needed to fit the persistent emission of the AXPs: given the narrow bandpass being fit, the convolution of two black bodies sometimes gives an acceptable fit in soft-spectrum sources (Israel et al. 2000). Measurements of the AXP emission above several keV are crucial to understanding the physical origin of the high energy excess.

16.7.4 *Torque Behavior*

In addition to the basic predictions of rapid spindown in the SGRs and bursting activity in the AXPs, theoretical work on magnetars has anticipated some other observed properties of the magnetar candidates. The deduction that the magnetic fields of the SGRs are time-variable suggested

that the spindown would also be highly variable (Thompson & Blaes 1998). If the magnetic field is variable on very short timescales, then torque variations will arise from a continuous flux of high frequency Alfvén waves and particles away from the star (see also Harding, Contopoulos, and Kazanas 1999; Thompson et al. 2000). This is the most plausible explanation for the transient spindown observed in SGR 1900+14 at the time of the 27 August 1998 flare. But the apparent time lag between bursting activity and large torque variations in SGRs 1900+14 and 1806–20, the observation of long-term ($>$ year) and persistent increases in torque, and the persistence of the changes in X-ray pulse profile following outbursts, are more consistent with the presence of large-scale currents on the closed magnetospheric field lines (Thompson et al. 2002). Torque variations could, in principle, also arise from a change in the fraction of open field lines due to the suspension of a modest amount of material inside the speed-of-light cylinder (Ibrahim et al. 2001); but it is difficult to see why such material would not be redistributed or expelled immediately following a bright SGR flare.

The magnetar model is conservative in the sense that the AXPs and SGRs are assumed to be standard neutron stars, distinguished only from radio pulsars (including the high-magnetic field tail of the pulsar population) by the presence of a strong wound-up magnetic field *inside* the star (Thompson & Duncan 2001), and by the active transfer of magnetic helicity across the stellar surface. One way of testing this basic hypothesis is to search for glitches associated with a superfluid component. Large glitches will be triggered in slowly rotating magnetars via the release of magnetic stresses in the crust – either due to sudden unpinning (Thompson & Duncan 1993) or to plastic deformations of the crust during which vortices remain pinned (Thompson et al. 2000). In the second case, spindown of the superfluid occurs if the crust is twisted adiabatically about an axis that is tilted with respect to the rotation axis: more superfluid vortices move outward away from the rotation axis than move toward it. A large glitch observed in the AXP 1E 2259+586 (Kaspi et al. 2003; Woods et al. 2004) provides a nice test of these ideas. The year-long soft X-ray afterglow observed following the glitch suggests that the crust was subject to a smooth, large-scale deformation. Related effects occurring in a superfluid core have also been implicated in the fast timing noise of the SGRs (Arras et al. 2004).

16.8 Future Directions

We close by outlining some major unsolved problems associated with the SGRs and AXPs.

[1] *What is the birth rate of AXPs and SGRs compared with radio pulsars? What fraction of neutron stars go through a phase of strong magnetic activity?* The selection of magnetar candidates – through their burst activity as SGRs, or through their persistent X-ray pulsations as AXPs – is limited by sensitivity. There are ~ 10 magnetar candidates in our Galaxy and a conservative estimate of their average age is $\sim 10^4$ years as derived from their spindown. Thus, a *lower limit* to the Galactic birth rate is 1 per 1000 years, or $\sim 10\%$ of the radio pulsar birth rate (Lyne et al. 1998). The birth rate that we infer for AXPs and SGRs depends critically upon the efficiency with which we detect them. The efficiency of detecting low-luminosity bursts such as those from 1E 2259+586 is quite low. The overall efficiency of identifying magnetar candidates has not yet been quantified. The observation of transitions to persistent low-luminosity states suggests that it may be lower than previously thought; but these transient sources could be older on average than the more persistent sources. Given the number of selection effects, we cannot rule out a detection efficiency as low as $\sim 10\%$, and a birth rate comparable to that of radio pulsars.

[2] *Why are the spin periods of AXPs and SGRs strongly clustered in an interval of 5 – 12 s?* This clustering suggests a real upper cutoff of ~ 12 s in the period distribution (Psaltis & Miller 2002). In fact, the observed periods lie close to the upper envelope of the period distribution of radio pulsars, and are consistent with a reduction in torque following the termination of active pair cascades on open magnetic field lines (Thompson et al. 2002). Field decay could, in principle, also play a role in determining the observed range of spin periods (Colpi et al. 2000). The large $\sim 2 \times 10^5$ yr characteristic age of 1E 2259+586 (which resides in the $\sim 10^4$ -yr old SNR CTB 109) provides a strong hint of torque decay in that particular AXP.

[3] *Do the SGRs, AXPs and high B-field radio pulsars form a continuum of magnetic activity, or are they different phases/states of a more uniform class of object?* The heating of a neutron star by a decaying magnetic field is unfortunately sensitive to the configuration of the field. Arras et al. (2004) consider a toroidal configuration, and show that as the field strength is reduced from $\sim 10^{15}$ G down to $\sim 10^{14}$ G, the soft X-ray luminosity interpolates between the levels characteristic of AXPs and of radio pulsars. Thus the observed X-ray emission of middle-aged radio pulsars is consistent with the hypothesis that the AXPs and SGRs have much stronger internal magnetic fields. However, a few AXPs have shown transitions to low-luminosity states where their X-ray output is reduced by a factor ~ 100 on a time scale of years. Much further exploration of the interplay between magnetic field transport, surface cooling, and superfluidity is required. For example, the

relaxation of the crustal magnetic field caused by electron captures on the heavy nuclei in the neutron-drip solid has not yet been explored.

[4] *What can we learn of neutron star matter from observations of SGR and AXP activity? Are SGRs and AXPs fundamentally neutron stars?* The detection of glitches in two AXPs indicates the presence of a superfluid component, whose pinning behavior (as deduced from the post-glitch response) is similar to that observed in radio pulsars. Burst afterglows have the potential to probe the outer layers of magnetars. Lyubarsky et al. (2002) argue that the extended afterglow observed following the 27 August 1998 flare is more consistent with the strongly stratified outer crust of a neutron star, than it is with a nearly constant density quark star. It has been suggested that the high luminosities of SGR flares are a result of QCD confinement near the surface of a bare quark star (Usov 2001); but the theoretical motivation for such objects is problematic (e.g. Akmal et al. 1998).

[5] *What is the initial spin period of magnetars? Could some magnetars (with millisecond periods) be connected to GRBs?* It is not known whether magnetars and radio pulsars are distinguished by the initial rotation of the neutron star, or alternatively by the stability properties of the magnetic field. It is possible that all nascent neutron stars develop $\sim 10^{15}$ G magnetic fields through fluid instabilities; but it is also likely that the large-scale order of the magnetic field is correlated with the speed of the rotation. For example, a large-scale helical dynamo is possible when the rotation period is comparable to the timescale of the convective motions, which is ~ 3 ms for Ledoux convection during the 10-s Kelvin phase of the neutron star (Duncan & Thompson 1992). This led to the prediction of a class of energetic supernovae in which the neutron core deposits $\sim 10^{51} - 10^{52}$ ergs of rotational energy by magnetic dipole radiation and later forms a strongly magnetic stellar remnant. The spin energy can be tapped even on the short timescale for the shock to emerge from a compact CO core, when the effects of a neutrino-driven wind are taken into account (Thompson, Chang & Quataert 2004). Whether a proto-magnetar is also a viable source of gamma-ray burst emission (as suggested independently by Usov 1992 and Duncan & Thompson 1992) is more problematic: the net mass released during neutrino cooling is a few orders of magnitude larger than what will quench gamma-ray emission from the expanding relativistic wind.

[6] *What is the evolutionary sequence of magnetars? How do very young ($< 10^3$ years) and older systems ($> 10^5$ years) manifest themselves? Are there old magnetars in our local neighborhood? in globular clusters?* The limited $\sim 10^4$ yr lifetime of SGR flare activity is a significant constraint on models of magnetic field decay. This lifetime is determined by the microscopic

transport processes acting on the magnetic field; *and* by the manner in which the star falls out of magnetostatic equilibrium – about which little is presently understood. Hall drift is not sensitive to temperature and can, for that reason, continue to power a low level of X-ray emission ($\sim 10^{33}$ erg s^{-1}) at an age of $\sim 10^6$ yrs. Rotational energy deposition also becomes more significant at lower flux levels (e.g. Ruderman et al. 1998). Evidence has recently been found for broad absorption features in the spectra of a few soft-spectrum Dim Isolated Neutron Stars (van Kerkwijk et al. 2004; Haberl 2004) perhaps indicative of proton cyclotron absorption in a magnetic field of several $\times 10^{13}$ G (Zane et al. 2001; Ho & Lai 2003; Özel 2003). Their evolutionary relation to radio pulsars and magnetars would be elucidated by a detailed cross comparison with the low-luminosity states of magnetars. Detailed timing measurements are likely to be essential to unravelling these interconnections.

[7] *Do magnetars exist in binary systems? If so, how does a magnetar react to accretion? Or, alternatively, do magnetars form only through the sacrifice of a binary companion?* The modest number of binary neutron stars which may have 10^{14} G magnetic fields (e.g. GX 1+4, 2S 0114+650; Li & van den Heuvel 1999) is probably inconsistent with a magnetar birth exceeding ~ 10 percent of the total neutron star birth rate, unless the magnetars have systematically larger kicks or their dipole fields decay significantly above an age of $\sim 10^5$ yrs. There is some evidence for large kicks in SGRs 0525–66 and 1900+14 (Cline et al. 1982; Thompson et al. 2000), but not in any of the AXPs. The limited $\sim 10^4$ yr lifetime of AXPs as bright X-ray sources makes it unlikely to see bright thermal X-ray emission from magnetars formed in high-mass binaries.

16.9 Acknowledgments

We thank Shri Kulkarni for his help and advice in planning this review, and Robert Duncan, Fotis Gavriil, and Marten van Kerkwijk for comments.

References

- Adler, S.L., Ann. Phys. 67, 599
 Akerlof, C., et al. 2000, ApJ, 542, 251
 Akmal, A., Pandharipande, V. R., & Ravenhall, D. G. 1998, Phys. Rev. C, 58, 1804
 Alcock, C., Farhi, E. & Olinto, A. 1986, Phys. Rev. Lett. 57, 2088
 Ardelyan, N. V., et al. 1987, Soviet Astr., 31, 398
 Aptekar, R.L., et al. 2001, ApJ, 137, 227
 Arras, P., Cumming, A., & Thompson, C. 2004, ApJ, 608, L49

- Arzoumanian, Z., Nice, D.J., Taylor, J.H. & Thorsett, S.E. 1994, *ApJ*, 422, 671
- Atteia, J.L., et al. 1987, *ApJ*, 320, L105
- Baade, W. & Zwicky, F. 1934, *Proc. Nat. Acad. Sci.* 20, 259
- Baykal, A. & Swank, J. 1996, *ApJ*, 460, 470
- Blaes, O., Blandford, R.D., Goldreich, P., & Madau P. 1989, *ApJ*, 343, 839
- Camilo, F., et al. 2000, *ApJ*, 541, 367
- Chatterjee, P., Hernquist, L., & Narayan, R. 2000, *ApJ*, 534, 373
- Chatterjee, P. & Hernquist, L. 2000, *ApJ*, 543, 368
- Cheng, B., Epstein, R.I., Guyer, R.A., & Young, C. 1996, *Nature*, 382, 518
- Cline, T.L., et al. 1982, *ApJ*, 255, L45
- Cline, T.L., et al. 2000, *ApJ*, 531, 407
- Colpi, M., Geppert, U., & Page, D. 2000, *ApJ*, 529, L29
- Corbel, S., Chapuis, C., Dame, T.M., & Durouchoux, P. 1999, *ApJ*, 526, L29
- Corbel, S. & Eikenberry, S.S. 2004, *A&A*, 419, 191
- Corbet, R.H.D., et al. 1995, *ApJ*, 443, 786
- Dall'Osso, S., et al. 2003, *ApJ*, 499, 485
- Duncan, R. & Thompson, C. 1992, *ApJ*, 392, L9
- Duncan, R. 2001, in 20th Texas Symp. on Relativistic Astrophysics, Eds. J.C. Wheeler & H. Martel, *AIP*, vol 586, pp. 495
- Durant, M., van Kerkwijk, M.H., & Hulleman, F. 2003, in Young Neutron Stars and their Environment: IAU Symp. 218, Eds. F. Camillo & B.M. Gaensler, p. 251 ([astro-ph/0309801](#))
- Eikenberry, S.S., et al. 2001, *ApJ*, 563, L133
- Fahlman G.G. & Gregory, P.C. 1981, *Nature*, 293, 202
- Fenimore, E.E., et al. 1981, *Nature*, 289, 42
- Fenimore, E., Laros, J.G., & Ulmer, A. 1994, *ApJ*, 432, 742
- Feroci, M., et al. 1999, *ApJ*, 515, L9
- Feroci, M., Hurley, K., Duncan, R.C. & Thompson, C. 2001, *ApJ*, 549, 1021
- Feroci, M., et al. 2003, *ApJ*, 596, 470
- Feroci, M., et al. 2004, *ApJ*, in press ([/astro-ph/0405104](#))
- Frail, D., Kulkarni, S. & Bloom, J. 1999, *Nature*, 398, 127
- Fuchs, Y., et al. 1999, *A&A*, 350, 891
- Gaensler, B.M. & Johnston, S. 1995, *MNRAS*, 277, 1243
- Gaensler, B.M., Gotthelf, E.V., & Vasisht, G. 1999, *ApJ*, 526, L37
- Gaensler, B.M., Slane, P.O., Gotthelf, E.V., & Vasisht, G. 2001, *ApJ*, 559, 963
- Gavriil, F. & Kaspi, V.M. 2002, *ApJ*, 567, 1067
- Gavriil, F. P., Kaspi, V. M., & Woods, P. M. 2002, *Nature*, 419, 142
- Gavriil, F. P., Kaspi, V. M., & Woods, P. M. 2004, *ApJ*, 607, 959
- Gavriil, F. & Kaspi, V.M. 2004, *ApJ*, in press ([astro-ph/0404113](#))
- Gnedin, O. Y., Yakovlev, D. G., & Potekhin, A. Y. 2001, *MNRAS*, 324, 725
- Göğüş, E., et al. 1999, *ApJ*, 526, L93
- Göğüş, E., et al. 2001, *ApJ*, 558, 228
- Göğüş, E., et al. 2002, *ApJ*, 577, 929
- Goldreich, P. & Reisenegger, A. 1992, *ApJ*, 395, 250
- Golenetskii, S.V., Ilyinskii, V.N., Mazets, E.P. 1984, *Nature*, 307, 41
- Gotthelf, E.V. & Vasisht, G. 1998, *New Astr.*, 3, 293
- Gotthelf, E.V., et al. 2002, *ApJ*, 564, L31
- Gotthelf, E.V., Halpern, J.P., Buxton, M., & Bailyn, C. 2004, *ApJ*, 605, 368
- Gregory, P.C. & Fahlman, G.G. 1980, *Nature*, 287, 805
- Guidorzi, C., et al. 2004, *A&A*, 416, 297

- Haberl, F. 2004, *Mem. S. A. It.*, 75, 454
- Haensel, P., Urpin, V.A., & Iakovlev, D.G. 1990, *A&A*, 229, 133
- Harding, A.K., Contopoulos, I., & Kazanas, D. 1999, *ApJ*, 525, L125
- Hellier, C. 1994, *MNRAS*, 271, L21
- Hewish, A., et al. 1968, *Nature*, 217, 709
- Heyl, J. S. & Hernquist, L. 1998, *MNRAS*, 300, 599
- Heyl, J. S. & Kulkarni, S. R. 1998, *ApJ*, 506, L61
- Heyl, J.S. & Hernquist, L. 1999, *MNRAS*, 304, L37
- Ho, W.C.G. & Lai, D. 2003, *MNRAS*, 338, 233
- Hulleman, F., et al. 2001, *ApJ*, 563, L49
- Hulleman, F., van Kerkwijk, M.H. & Kulkarni, S.R. 2000, *Nature*, 408, 689
- Hulleman, F., van Kerkwijk, M.H. & Kulkarni, S.R. 2004, *A&A*, 416, 1037
- Hurley, K. 1986, Talk presented at the Gamma-Ray Stars Conference in Taos, NM
- Hurley, K.J., McBreen, B., Rabbette, M., & Steel, S. 1994, *A&A*, 288, L49
- Hurley, K., et al. 1999a, *Nature*, 397, 41
- Hurley, K., et al. 1999b, *ApJ*, 510, L107
- Hurley, K., et al. 1999c, *ApJ*, 510, L111
- Hurley, K., et al. 1999d, *ApJ*, 523, L37
- Ibrahim, A., et al. 2001, *ApJ*, 558, 237
- Ibrahim, A.I., Swank, J.H., & Parke, W. 2003, *ApJ*, 584, L17
- Ibrahim, A.I., et al. 2004, *ApJ*, submitted, ([astro-ph/0310665](#))
- Inan, U.S., et al. 1999, *GeorL*, 26, 3357
- Israel, G.L., et al. 2000, *ApJ*, 560, L65
- Israel, G.L., et al. 2002, *ApJ*, 580, L143
- Israel, G.L., et al. 2003a, in *Young Neutron Stars and their Environment: IAU Symp. 218*, Eds. F. Camillo & B.M. Gaensler, in press, ([astro-ph/0310482](#))
- Israel, G.L., et al. 2003b, *ApJ*, 589, L93
- Israel, G.L., et al. 2004, *ApJ*, 603, L97
- Iwasawa, K., Koyama, K. & Halpern, J.P. 1992, *Publ. Astron. Soc. Japan*, 44, 9
- Jones, P. B. 2003, *ApJ*, 595, 342
- Juett, A.M., Marshall, H.L., Chakrabarty, D., & Schulz, N.S. 2002, *ApJ*, 568, L31
- Kaplan, D.L., et al. 2001, *ApJ*, 556, 399
- Kaplan, D.L., Kulkarni, S.R., Frail, D.A., & van Kerkwijk, M.H. 2002, *ApJ*, 566, 378
- Kaspi, V.M., Lackey, J.R., & Chakrabarty, D. 2000, *ApJ*, 537, L31
- Kaspi, V.M., et al. 2001, *ApJ*, 558, 253
- Kaspi, V.M., et al. 2003, *ApJ*, 588, L93
- Kaspi, V.M. & Gavriil, F.P. 2003, *ApJ*, 596, L71
- Katz, J.I., Toole, H.A., & Unruh, S.H. 1994, *ApJ*, 437, 727
- Kern, B. & Martin, C. 2002, *Nature*, 417, 527
- Klose, S., et al. 2004, *ApJ* in press ([astro-ph/0405299](#))
- Koshut, T.M., et al. 1996, *ApJ*, 463, 570
- Kothes, R., Uyaniker, B., & Aylin, Y. 2002, *ApJ*, 576, 169
- Kouveliotou, C., et al. 1987, *ApJ*, 322, L21
- Kouveliotou, C., et al. 1998, *Nature*, 393, 235
- Kouveliotou, C., et al. 2003, *ApJ*, 596, L79
- Koyama, K., Hoshi, R., & Nagase, F. 1987, *PASJ*, 39, 801
- Kuiper, L., Hermsen, W., & Mendez, M. 2004, *ApJ*, submitted, ([astro-ph/0404582](#))
- Kulkarni, S.R., et al. 2003, *ApJ*, 585, 948

- Lamb, D., et al. 2003a, GCN Circ. 2351
- Lamb, R.C., Fox, D.W., Macomb, D.J., & Prince, T.A. 2002, ApJ, 574, L29
- Lamb, D., Prince, T.A., Macomb, D.J., & Majid, W.A. 2003b, IAU Circ. 8220
- Laros, J., et al. 1987, ApJ, 320, L111
- LeBlanc, J.M. & Wilson, J.R. 1970, ApJ, 161, 541
- Lenters, G.T., et al. 2003, ApJ, 587, 761
- Li, X.-D. & van den Heuvel, E.P.J. 1999, ApJ, 513, L45
- Livio, M. & Taam, R.E. 1987, Nature, 327, 398
- Lyne, A.G., et al. 1998, MNRAS, 295, 743
- Lyubarskii, Y.E. 1987, Astrophysics, 25, 277
- Lyubarsky, Y. 2002, MNRAS, 332, 199
- Lyubarsky, E., Eichler, D., & Thompson, C. 2002, ApJ, 580, L69
- Lyutikov, M. 2003, MNRAS, 346, 540
- Manchester, R.N. 2004, Science, 304, 542
- Marsden, D. & White, N.E. 2001, ApJ, 551, L155
- Mazets, E.P., et al. 1979, Nature, 282, 587
- Mazets, E.P. & Golenetskii, S.V. 1981, Ap&SS, 75, 47
- Mazets, E.P., et al. 1999a, Astron. Lett., 25, 635
- Mazets, E.P., et al. 1999b, ApJ, 519, L151
- McLaughlin, M.A., et al. 2003, ApJ, 591, L135
- Mereghetti, S. & Stella, L. 1995, ApJ, 442, L17
- Mereghetti, S., Cremonesi, D., Feroci, M., & Tavani, M. 2000, A&A, 361, 240
- Mereghetti, S., et al. 2001, MNRAS, 321, 143
- Mereghetti, S., et al. 2004, ApJ, in press, ([astro-ph/0404193](#))
- Miller, M.C. 1995, ApJ, 448, L29
- Molkov, S.V., et al. 2004, Astr. Lett. in press, ([astro-ph/0402416](#))
- Morii, M., Sato, R., Kataoka, J., & Kawai, N. 2003, PASJ, 55, L45
- Murakami, T., et al. 1994, Nature, 368, 127
- Norris, J.P., Hertz, P., Wood, K.S., & Kouveliotou, C. 1991, ApJ, 366, 240
- Olive, J-F., et al. 2003, in Gamma-ray Burst and Afterglow Astronomy 2001, Eds. G.R. Ricker & R.K. Vanderspek, *AIP*, vol 662, pp. 82-87
- Oosterbroek, T., Parmar, A.N., Mereghetti, S., & Israel, G.L. 1998, A&A, 334, 925
- Özel, F. 2002, ApJ, 575, 397
- Özel, F. 2003, ApJ, 583, 402
- Özel, F., Psaltis, D. & Kaspi, V.M. 2001, ApJ, 563, 255
- Paczynski, B., 1990, ApJ, 365, L9
- Paczynski, B., 1992, Acta Astron., 42, 145
- Palmer, D. M. 1999, ApJ, 512, L113
- Palmer, D.M. 2002, in Soft Gamma Repeaters: The Rome 2001 Mini-Workshop, Eds. M. Feroci & S. Mereghetti, Mem. S. A. It., vol 73, n. 2, pp. 578-583
- Patel, S.K., et al. 2001, ApJ, 563, L45
- Patel, S.K., et al. 2003, ApJ, 587, 367
- Perna, R., Hernquist, L.E., & Narayan, R. 2000, ApJ, 541, 344
- Pethick, C.J. 1992, in Structure and Evolution of Neutron Stars, eds. D. Pines, R. Tamagaki, and S. Tsuruta, p. 115
- Pivovarov, M.J., Kaspi, V.M., & Camilo, F. 2000, ApJ, 535, 379
- Potekhin, A. Y. & Yakovlev, D. G. 2001, A&A, 374, 213
- Psaltis, D. & Miller, M.C. 2002, ApJ, 578, 325
- Ramaty, R., et al. 1980, Nature, 287, 122

- Rea, N., et al. 2003, ApJ, 586, L65
Rothschild, R., Kulkarni, S. & Lingefelter, R. 1994, Nature, 368, 432
Ruderman, M., Zhu, T., & Chen, K. 1998, ApJ, 492, 267
Shitov, Yu.P. 1999, IAU Circ. 7110
Symbalisty, E.M.D. 1984, ApJ, 285, 729
Sil'antev, N.A. & Iakovlev, D.G. 1980, Ap&SS, 71, 45
Strohmayer, T.E. & Ibrahim, A.I. 2000, ApJ, 537, L111
Terrell, J., Evans, W.D., Klebesadel, R.W., & Laros, J.G. 1980, Nature, 285, 383
Thompson, C., & Blaes, O. 1998, Phys. Rev. D, 57, 3219
Thompson C. & Duncan R.C. 1992, in Compton Gamma-Ray Observatory, eds.
M. Friedlander, N. Gehrels and D.J. Macomb (AIP: New York), p. 1085
Thompson, C., & Duncan, R. 1993, ApJ, 408, 194
Thompson, C., & Duncan, R. 1995, MNRAS, 275, 255
Thompson, C., & Duncan, R. 1996, ApJ, 473, 322
Thompson, C., et al. 2000, ApJ, 543, 340
Thompson, C., & Duncan, R. 2001, ApJ, 561, 980
Thompson, C., Lyutikov, M., & Kulkarni, S.R. 2002, ApJ, 574, 332
Thompson, T., Chang, P., & Quataert, E. 2004, ApJ, in press
(astro-ph/0401555)
Torii, K., Kinugasa, K., Katayama, K., & Tsunemi, H. 1998, ApJ 503, 843
Usov, V.V. 1992, Nature, 357, 472
Usov, V.V. 1994, ApJ, 427, 984
Usov, V. V. 2001, ApJ, 559, L135
van Kerkwijk, M. H., et al. 1995, ApJ, 444, L33
van Kerkwijk, M.A., et al. 2004, ApJ, in press (astro-ph/0402418)
van Paradijs, J., Taam, R.E. & van den Heuvel, E.P.J. 1995, A&A, 299, L41
van Riper, K. A. 1988, ApJ, 329, 339
Vasisht, G., Kulkarni, S., Frail, D. & Greiner, J. 1994, ApJ, 431, L35
Vasisht, G. & Gotthelf, E.V. 1997, ApJ, 486, L129
Vasisht, G., Gotthelf, E.V., Torii, K., & Gaensler, B.M. 2000, ApJ, 542, L49
Vrba, F.J., et al. 2000, ApJ, 533, L17
Wachter, S., et al. 2004, ApJ, submitted, (astro-ph/04mmnnn)
Wang, Z. & Chakrabarty, D. 2002, ApJ, 579, L33
Woltjer, L. 1964, ApJ, 140, 1309
Woods, P.M., et al. 1999a, ApJ, 519, L139
Woods, P.M., et al. 1999b, ApJ, 527, L47
Woods, P.M., et al. 1999c, ApJ, 524, L55
Woods, P.M., et al. 2000, ApJ, 535, L55
Woods, P.M., et al. 2001, ApJ, 552, 748
Woods, P.M., et al. 2002, ApJ, 576, 381
Woods, P.M., et al. 2003, ApJ, 596, 464
Woods, P.M. 2003, in Pulsars, AXPs, and SGRs Observed with *BeppoSAX* and
other Observatories, Eds. G. Cusumano, E. Massaro, & T. Mineo,
(Rome:Aracne), 159
Woods, P.M., et al. 2004, ApJ, 605, 378
Woosley, S.E. & Wallace, R.K. 1982, ApJ, 258, 716
Yakovlev, D. G., Kaminker, A. D., Gnedin, O. Y., & Haensel, P. 2001, Phys. Rep.,
354, 1
Zane, S., Turolla, R., Stella, L., & Treves, A. 2001, ApJ, 560, 384